kernel-phase for high angular resolution imaging

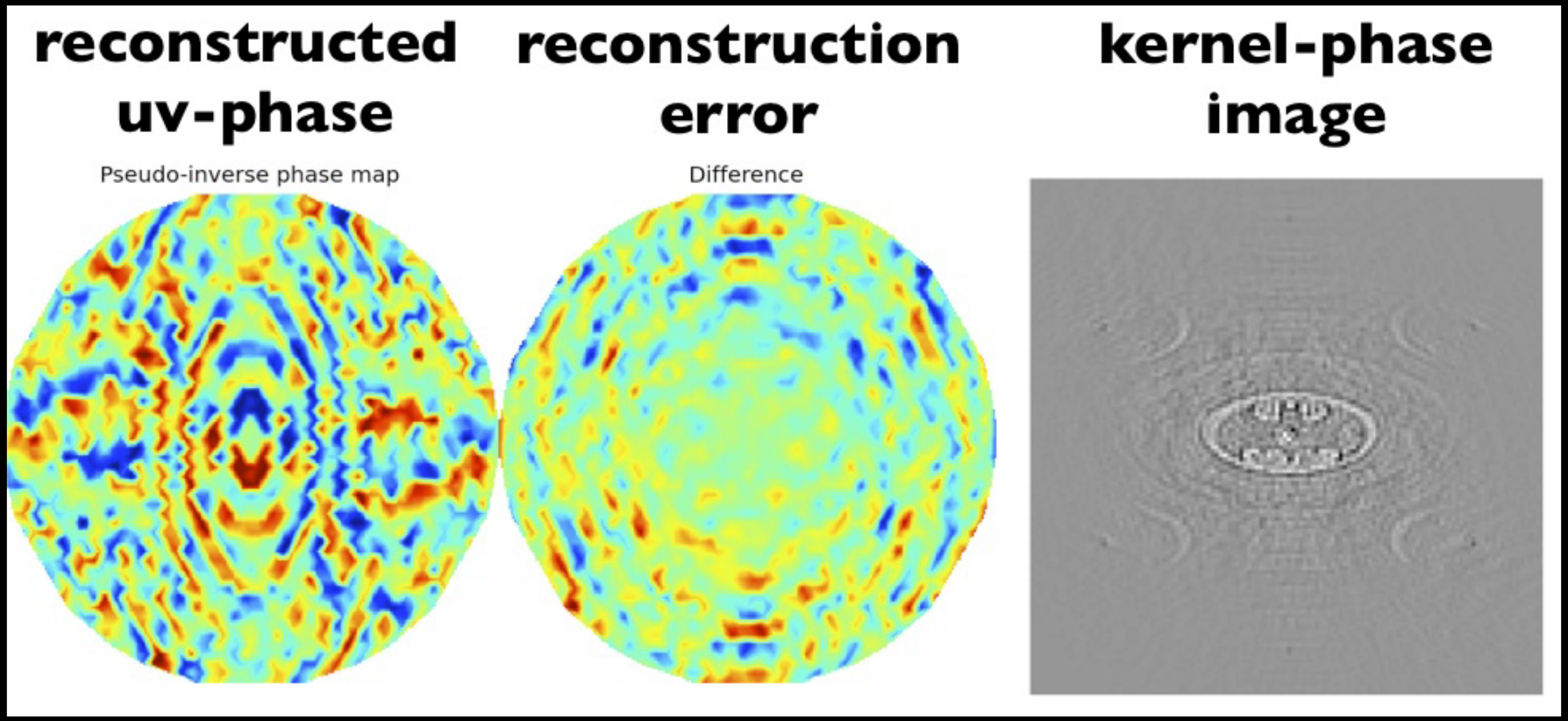

Frantz Martinache, Laboratoire Lagrange, OCA

+ B. Pope, P. Tuthill, M. Ireland, A. Cheetham, A. Latyshev, J. Monnier...

Strong legacy of the early days...

the 2-telescope interferometer remains the elementary brick of larger arrays

Lopez et al.

MATISSE:
- 4-beam combiner
- 6 baselines
- 3 closure triangles

Even rich recombiners ...

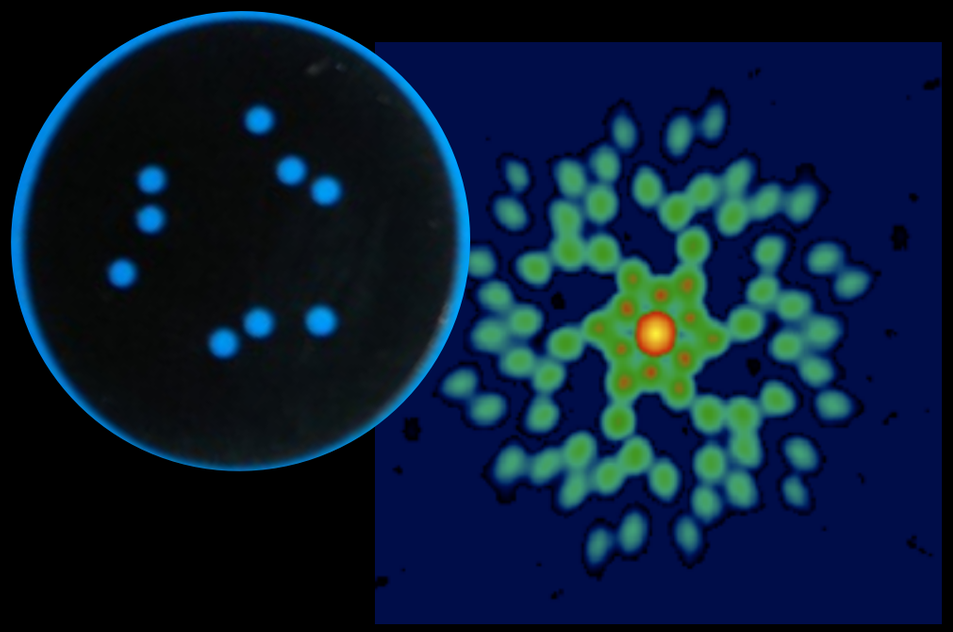

Aperture mask:
- 9-beam combiner
- 36 baselines
- 24 closure triangles

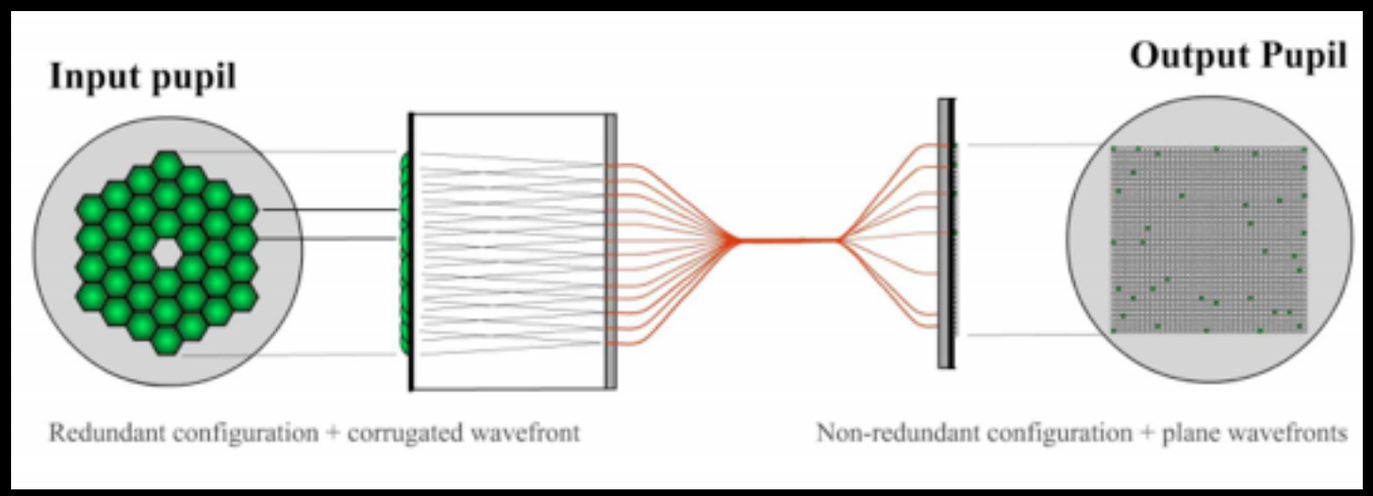

Perrin et al, 2006

FIRST:
- 36-beam combiner
- spatial filtering
- fiber remapping

... live under the rule of non-redundancy

To take advantage of self-calibration

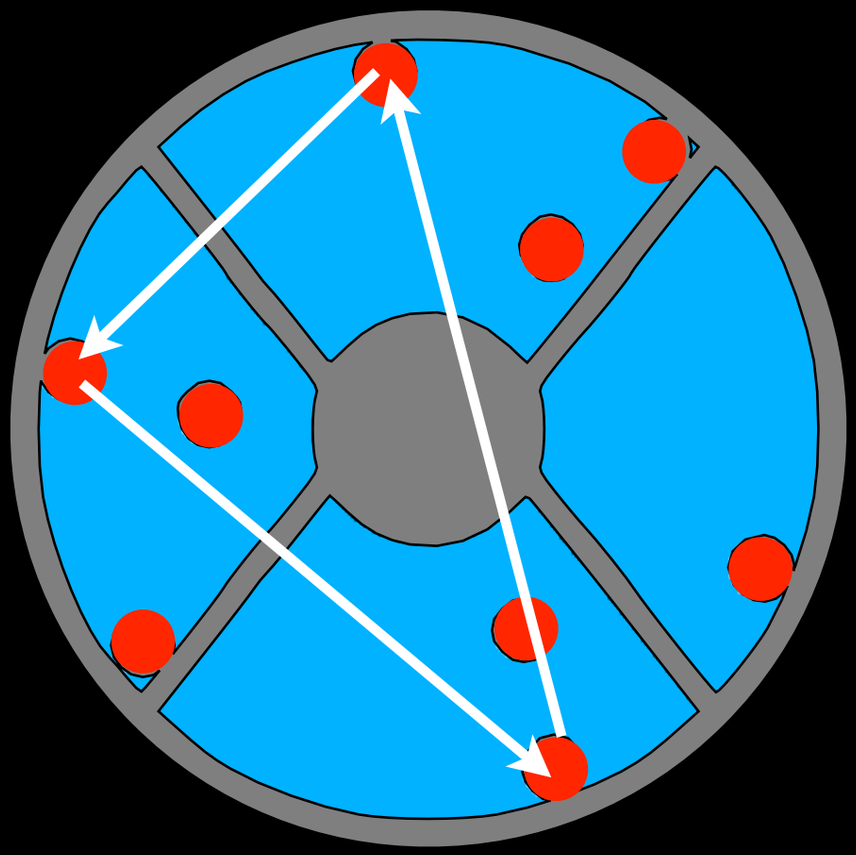

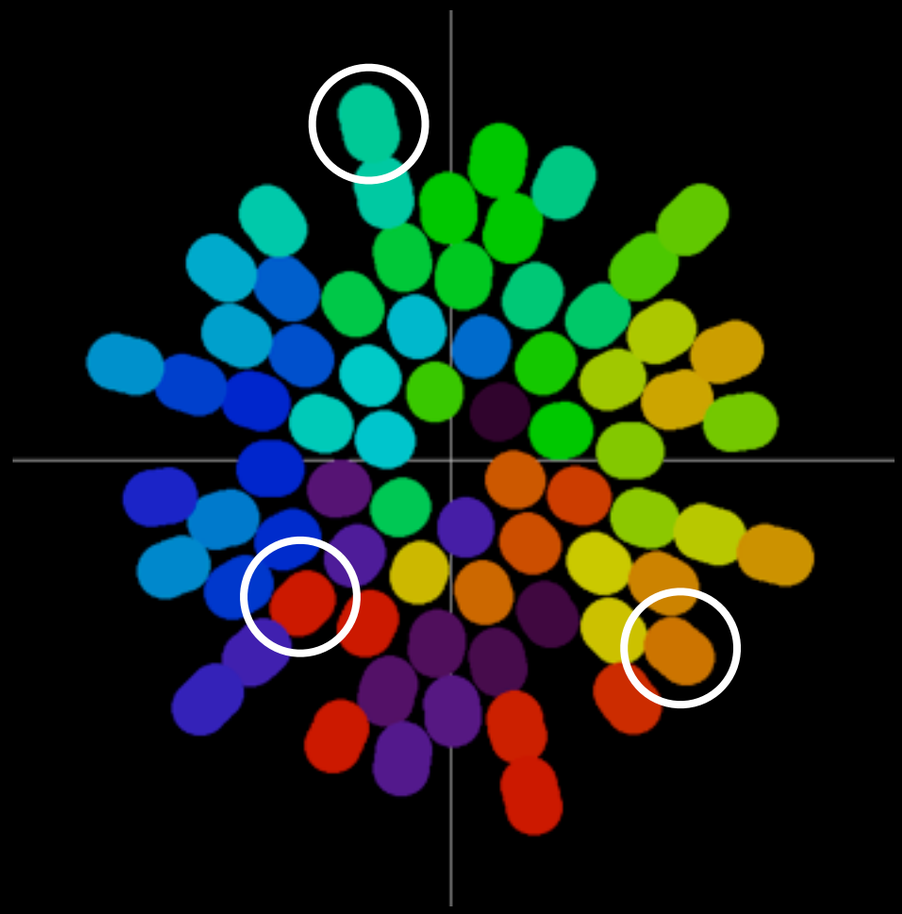

the closure-phase:

$$\Phi(1\text{-}2) = \Phi(1\text{-}2)_0 + (\Phi_1\text{-}\Phi_2)$$
$$\Phi(2\text{-}3) = \Phi(2\text{-}3)_0 + (\Phi_2\text{-}\Phi_3)$$
$$\Phi(3\text{-}1) = \Phi(3\text{-}1)_0 + (\Phi_3\text{-}\Phi_1)$$

Jennison, 1958, MNRAS, 118, 276

To what end?

1. High contrast detection near the diffraction limit

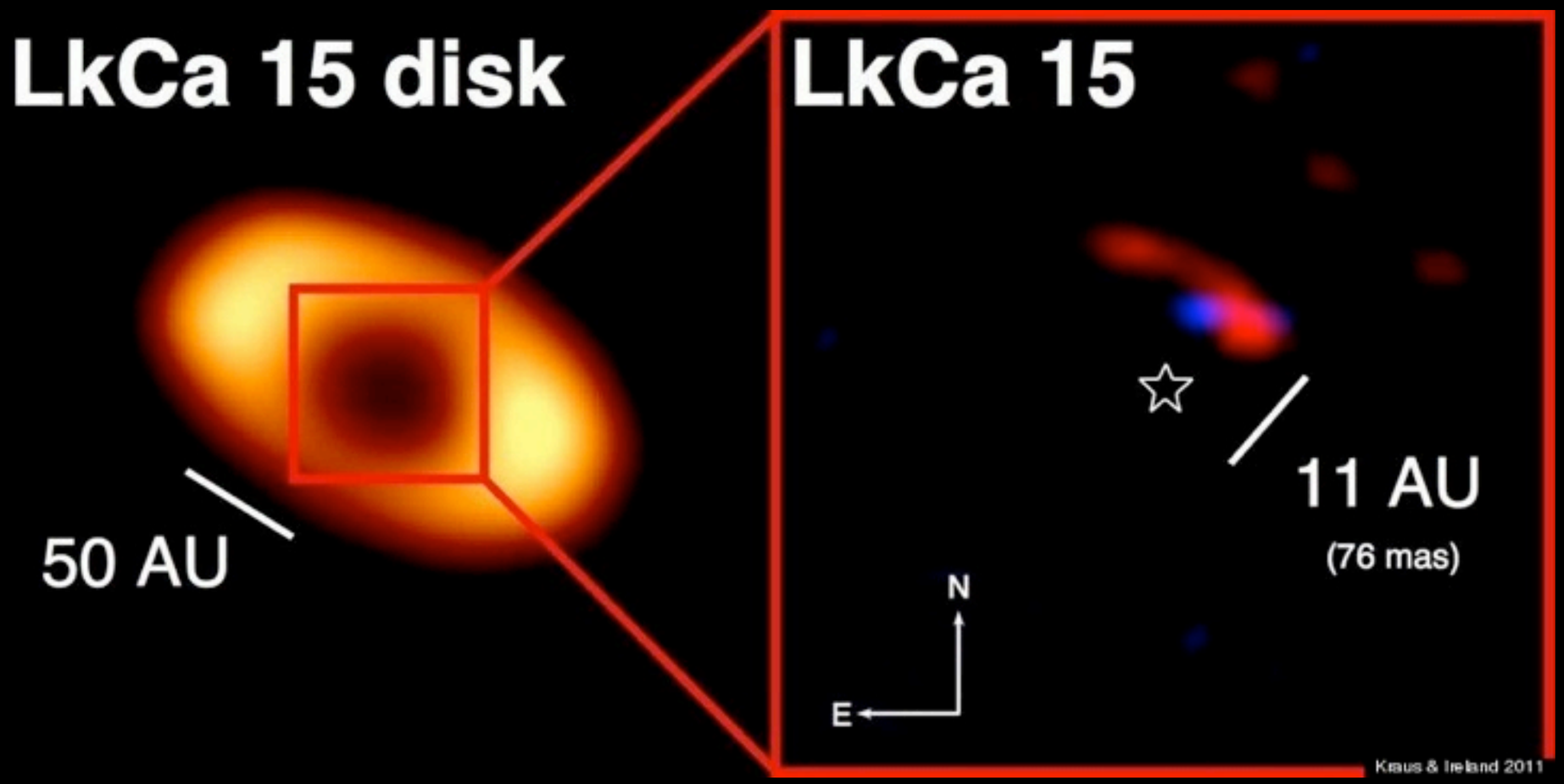

Kraus & Ireland, 2012, ApJ, 745, 5

The self-calibration properties of closure phase make NRM "bullet-proof"

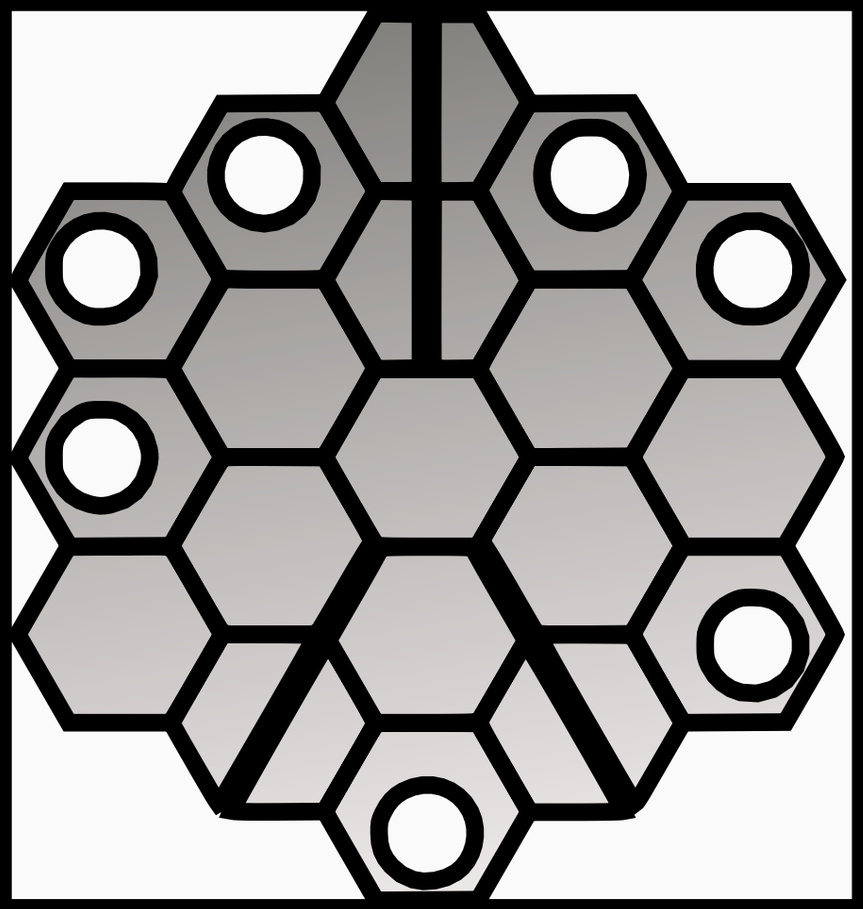

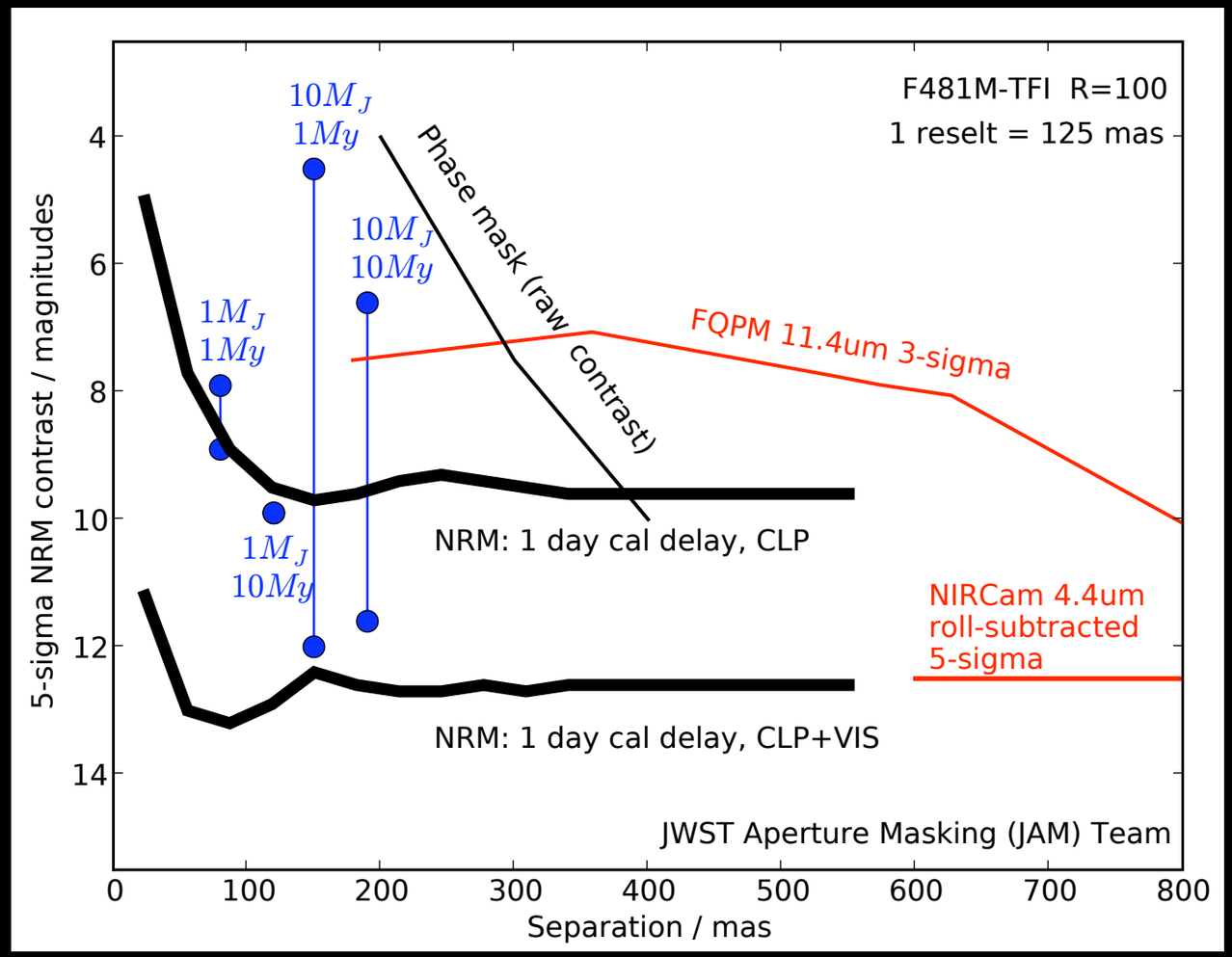

NRM onboard JWST in the NIRISS instrument.

Sivaramakrishnan et al, Astro2010T, 40

But very rich combiner exist...

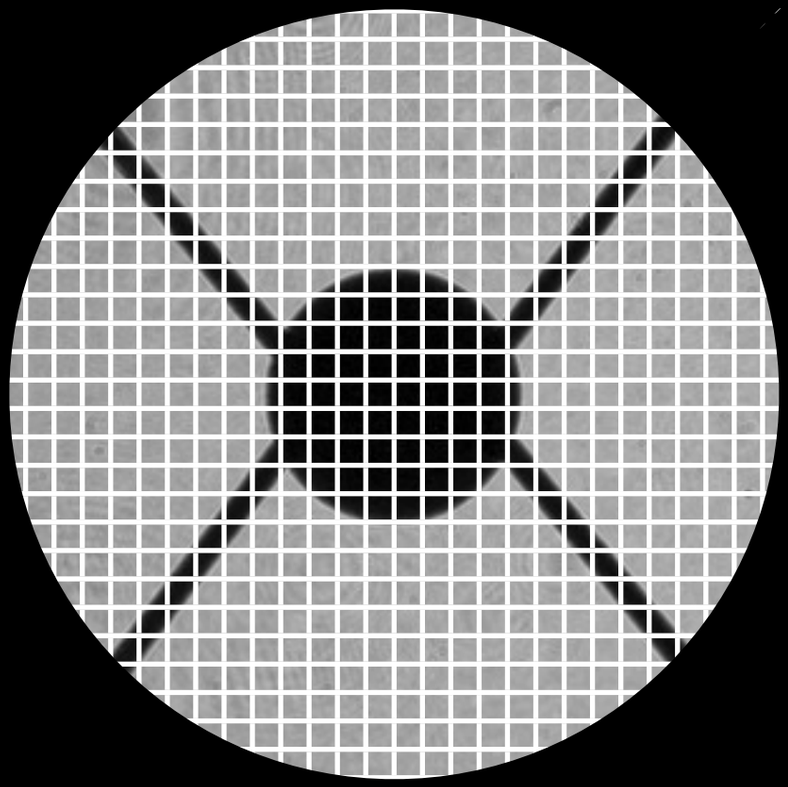

pupil

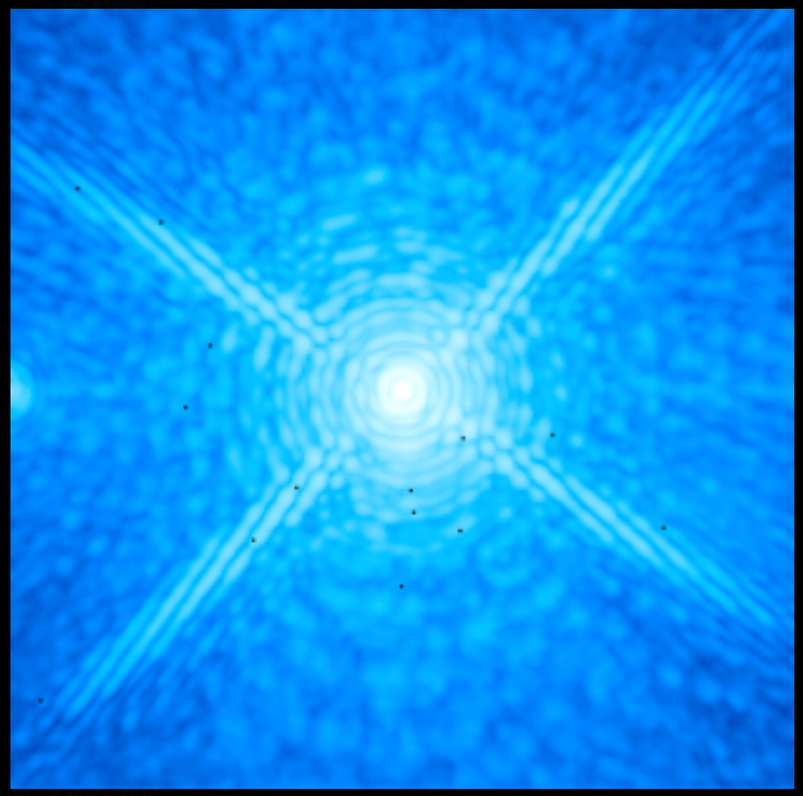

~~interferogram~~
image

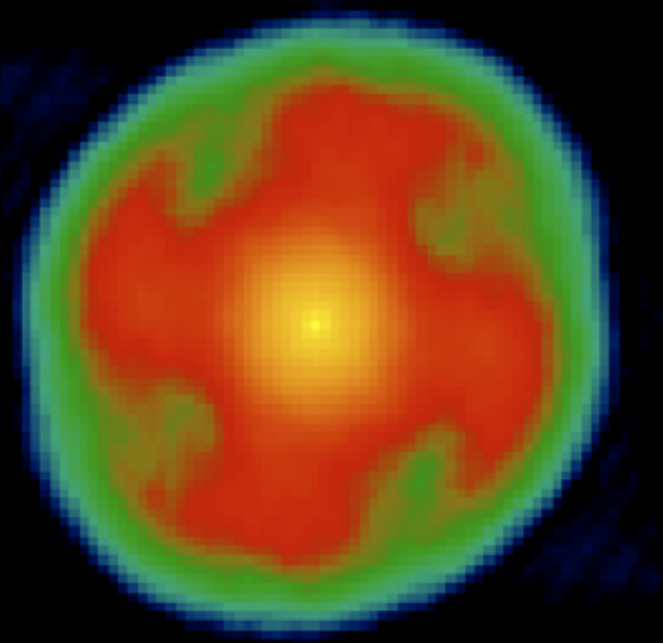

uv-plane

Redundancy rules

with AO, the phase can be linearized

non-redondant

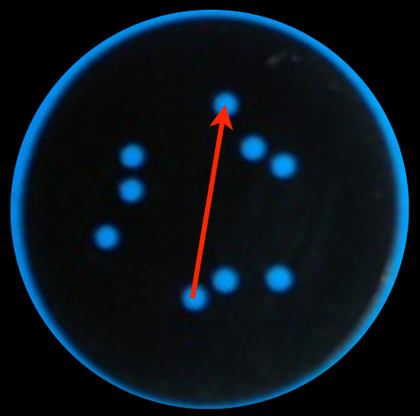

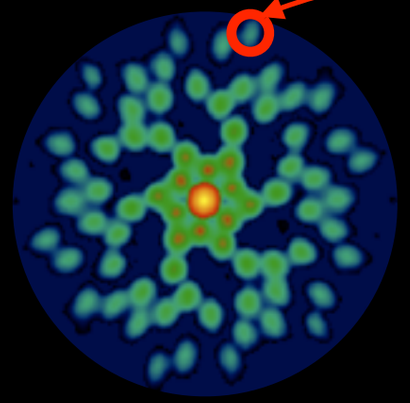

$\Phi_j = \Phi_{0j} + I\,\Delta\varphi$

full aperture

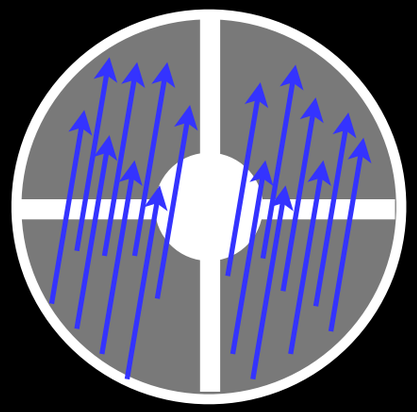

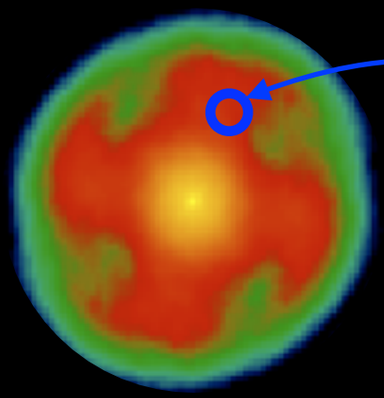

$\Phi_j = \Phi_{0j} + \mathrm{Arg}(\Sigma e^{j\,\Delta\varphi i})$

$\Phi_j = \Phi_{0j} + I/n_j\,\Sigma_i\,\Delta\varphi i$

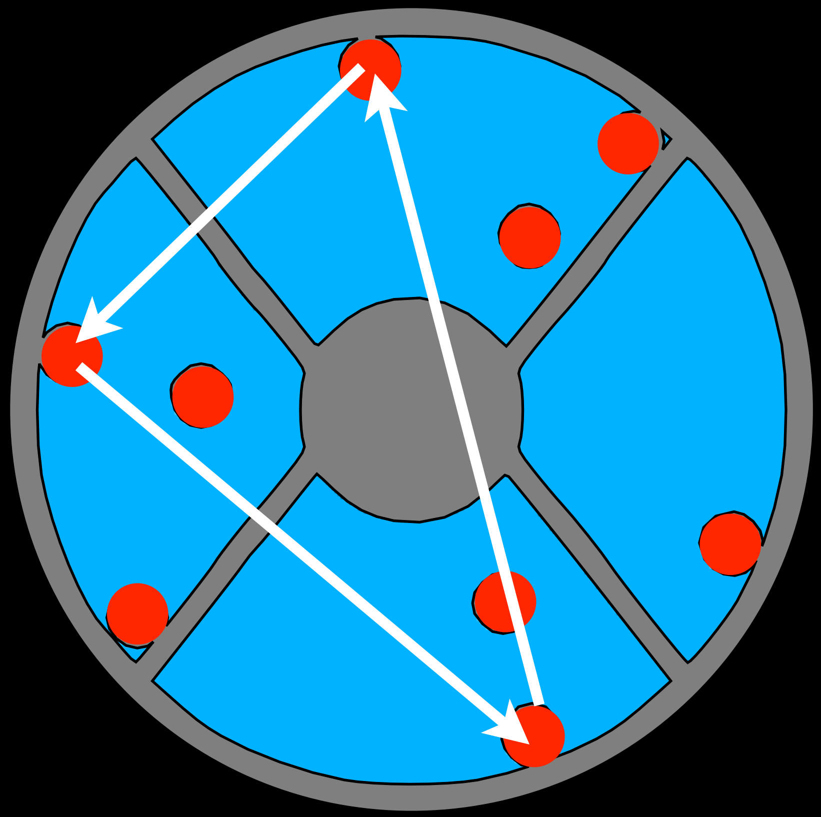

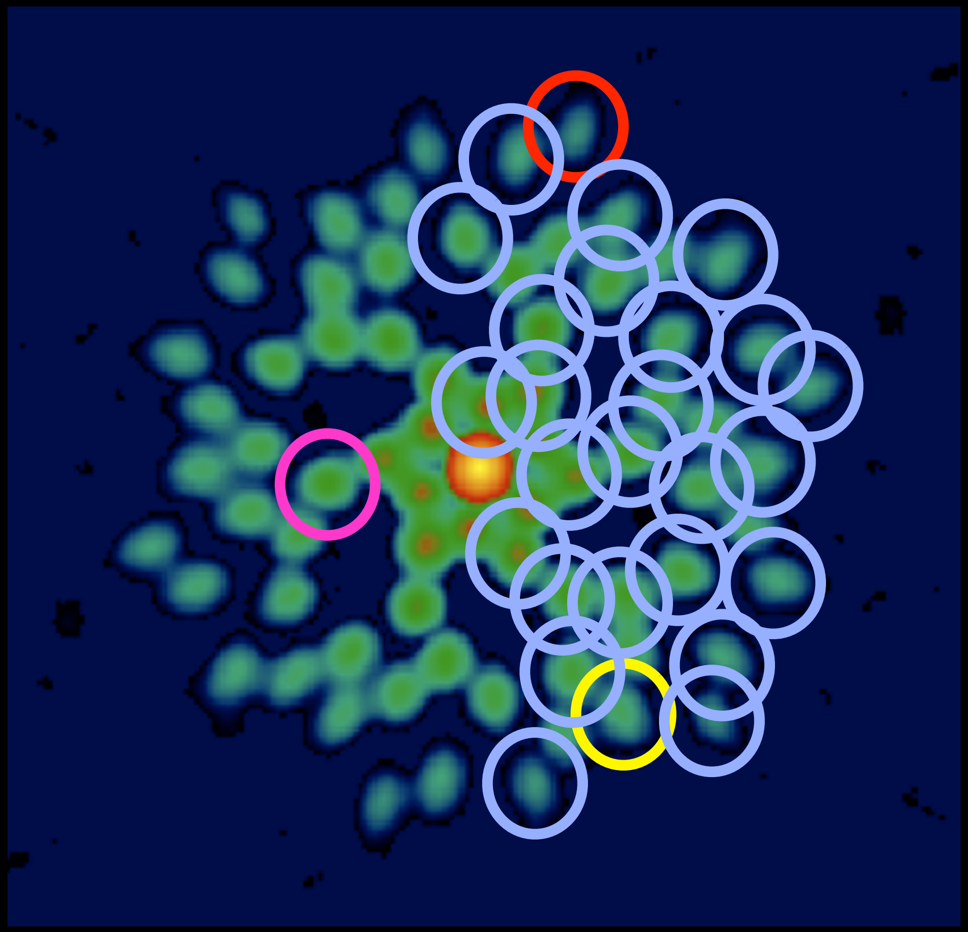

$\Phi(1\text{-}2) =$

$\Phi(2\text{-}3) =$

$\Phi(3\text{-}1) =$

$] \times [\,\varphi\,]$

$$[\,\Phi\,] = [\,\Phi_0\,] + [\,A\,] \times [\,\varphi\,]$$

measured Fourier phase	true Fourier phase	phase transfer matrix	pupil wavefront errors

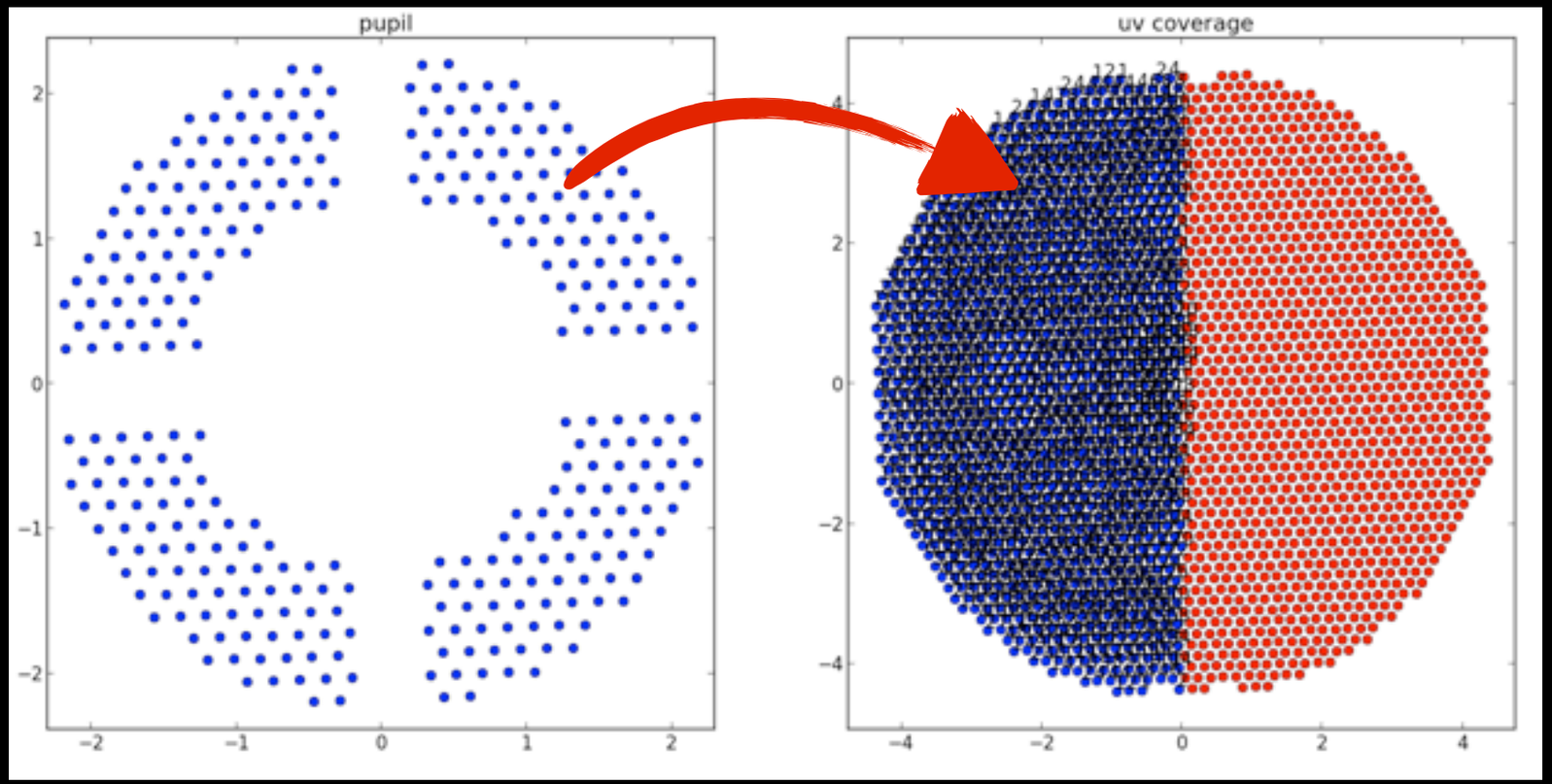

$$\begin{bmatrix} \Phi \end{bmatrix} = \begin{bmatrix} \Phi_0 \end{bmatrix} + \begin{bmatrix} A \end{bmatrix} \times \begin{bmatrix} \varphi \end{bmatrix}$$

measured

unknown

known

unknown

$$\Phi = \Phi_o + A.\varphi$$

$$K\,\phi = K\,\phi o + K\,A\,\varphi$$

$$K\,\phi = K\,\phi o$$

(*kernel-phase*)

$$\varphi = A^{-1} . (\phi - \phi_o)$$

(*eigen-phase*)

It is all about exploiting the properties of A

Martinache, 2010, ApJ, 724, 464

Martinache, 2013, PASP, 125, 422

FYI: cophasing JWST

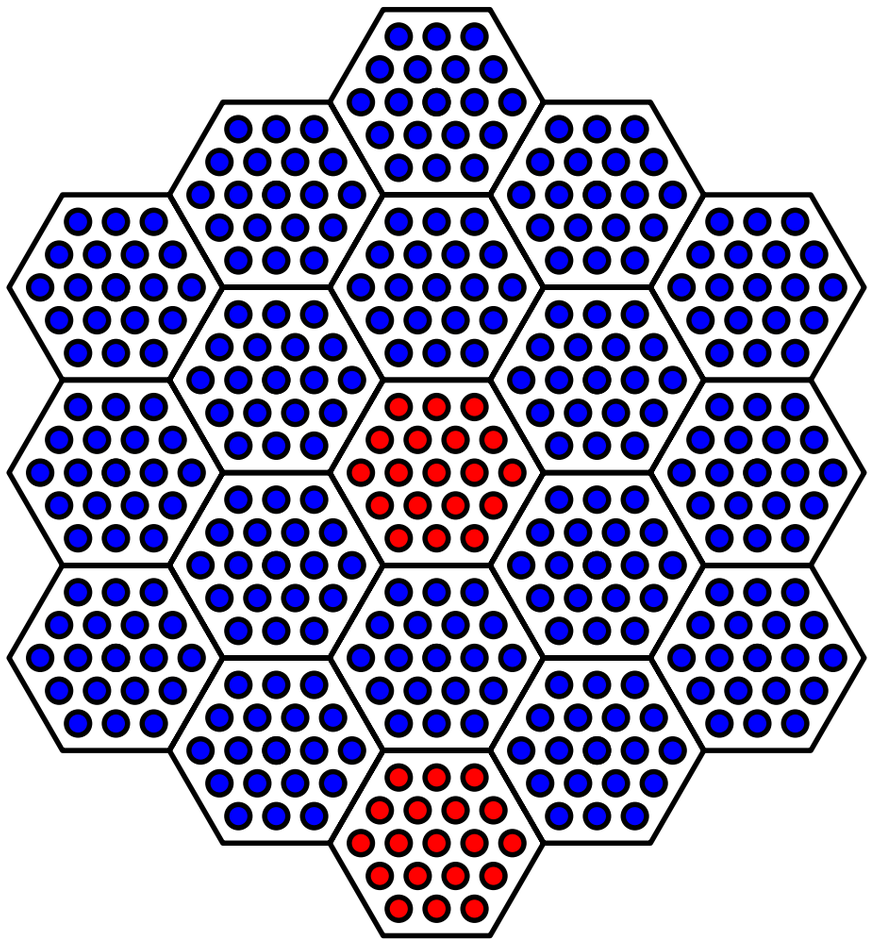

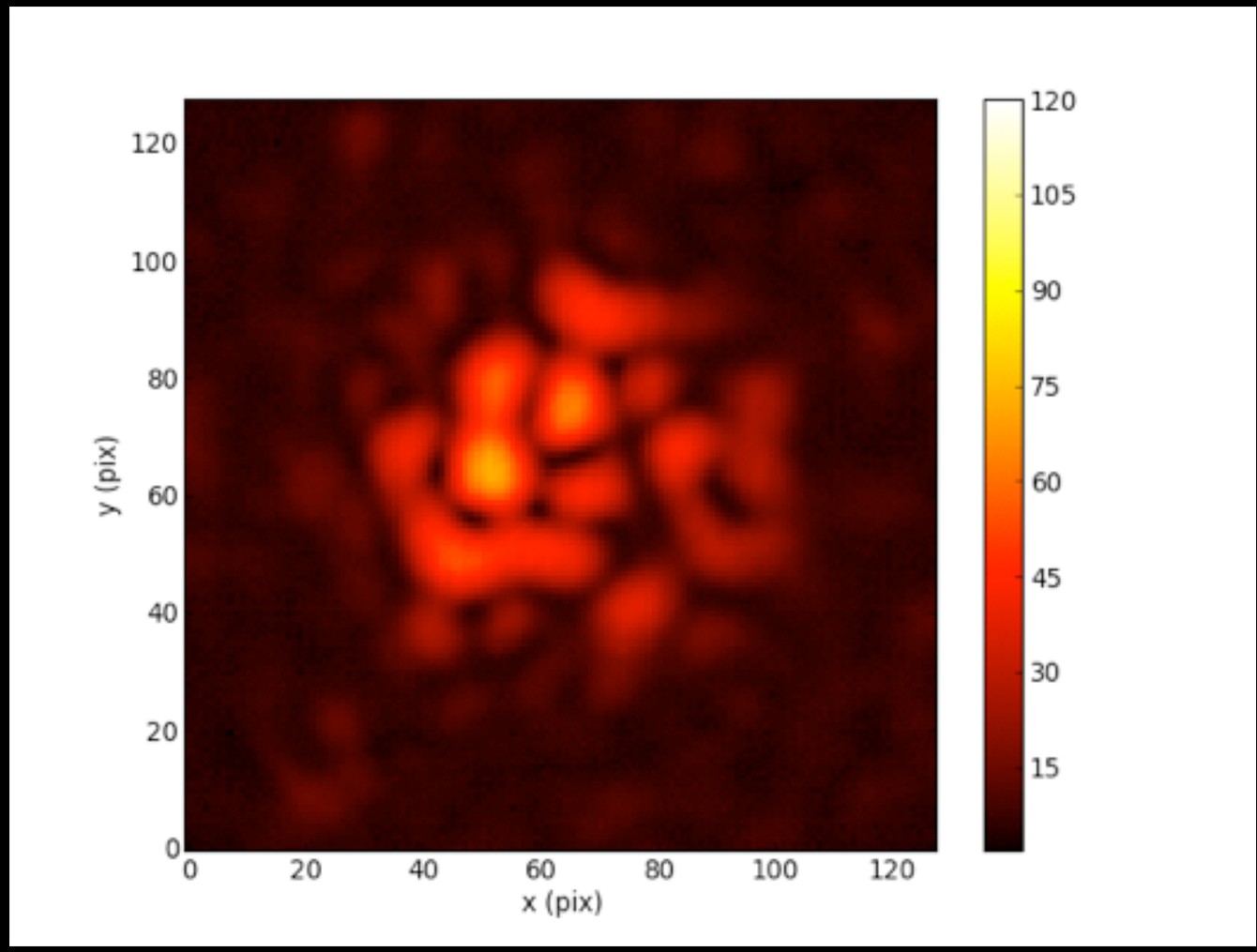

Pope et al, 2014, MNRAS, 440, 125

Data analysis

1. Build a instrument model => A
2. Find the Kernel of A: K

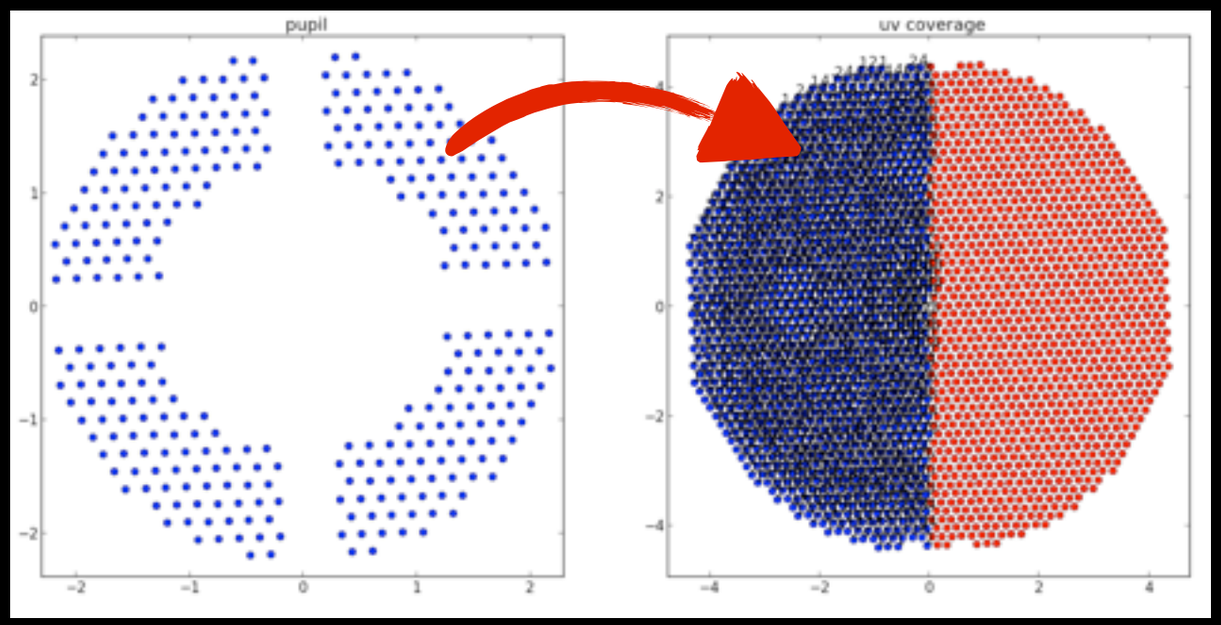

3. Fourier Transform each image
4. Extract phase ϕ

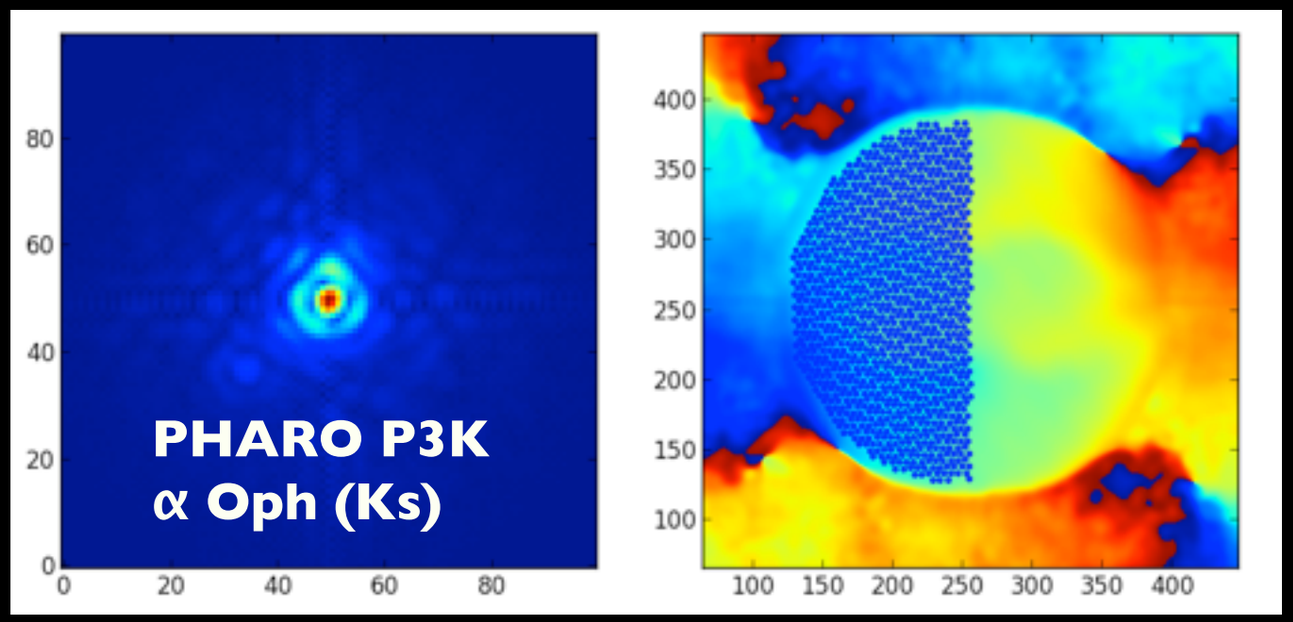

5. Multiply K ϕ: you are done!

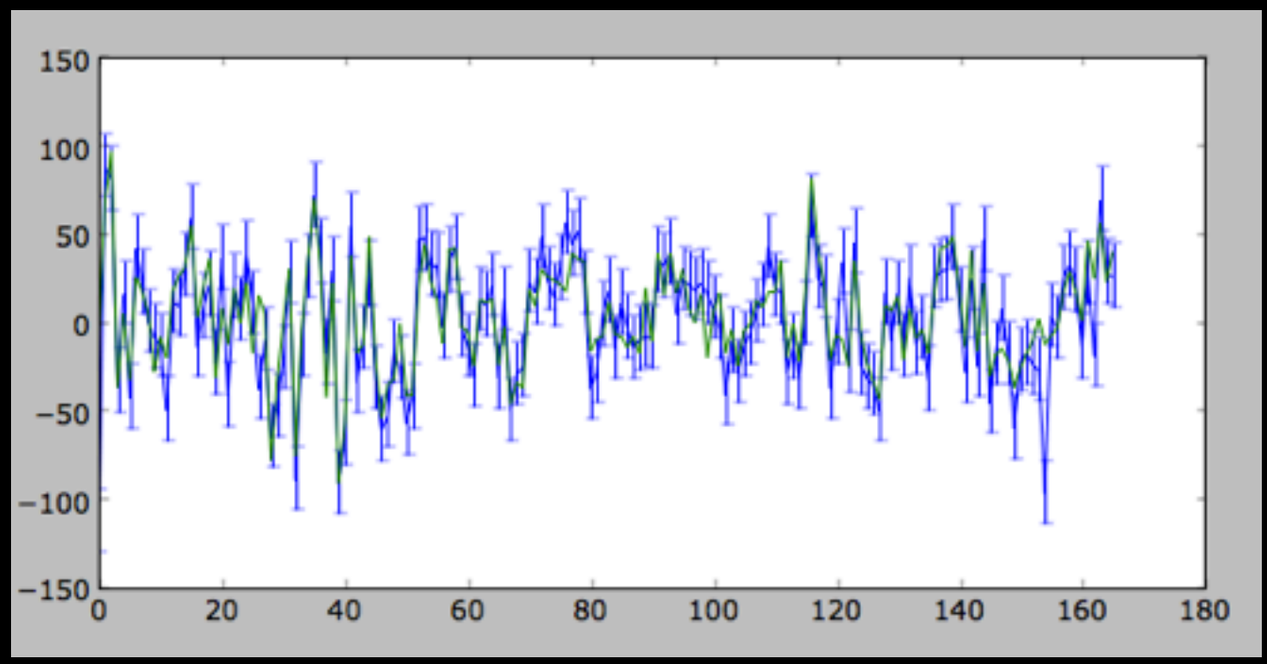

Additionally:
- statistics
- model the data (e.g. binary)
- determine contrast limits

http://code.google.com/p/pysco/

First ground based Ker-phase detection

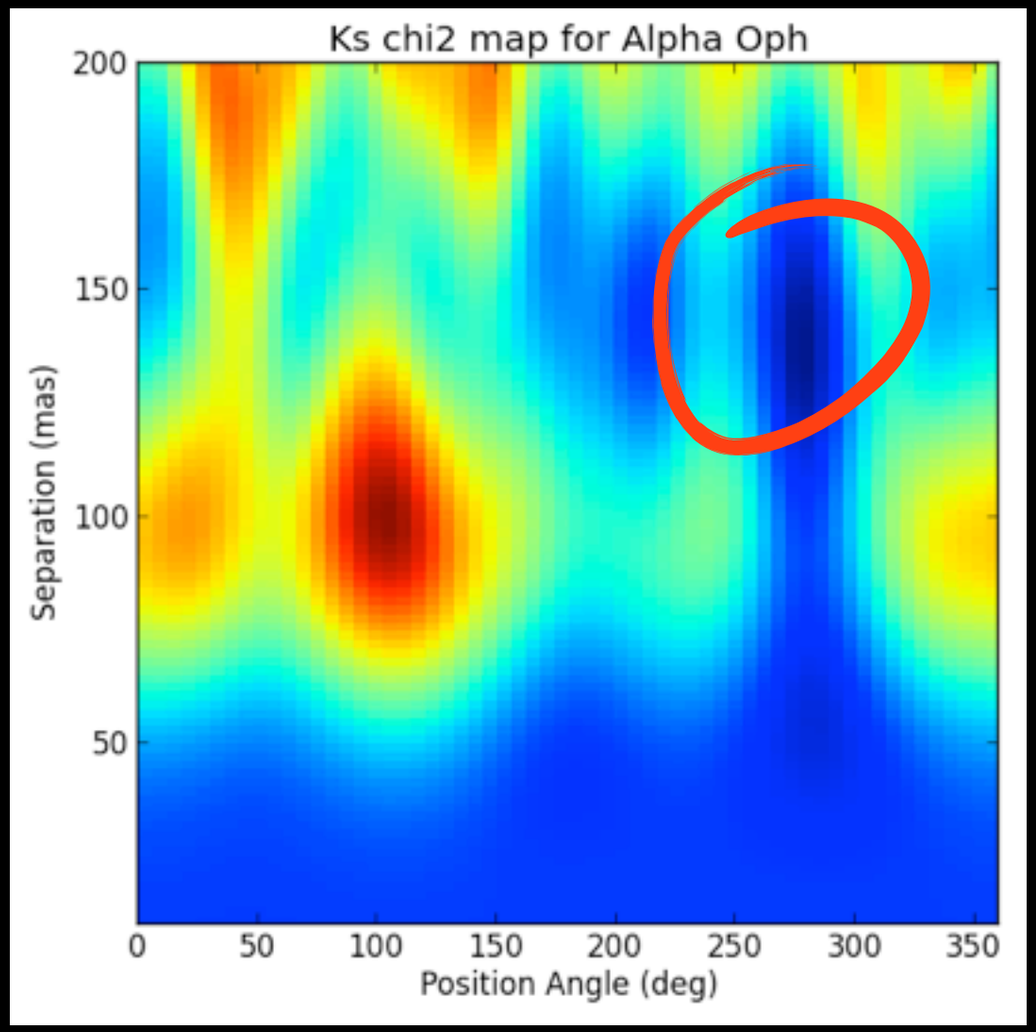

- Separation: 131.4 +/- 0.9 mas
- Position Angle: 86.0 +/- 0.2 deg
- Contrast: 19.7 +/- 0.4

Data, courtesy of S. Hinkley

Pope et al, 2015, in prep

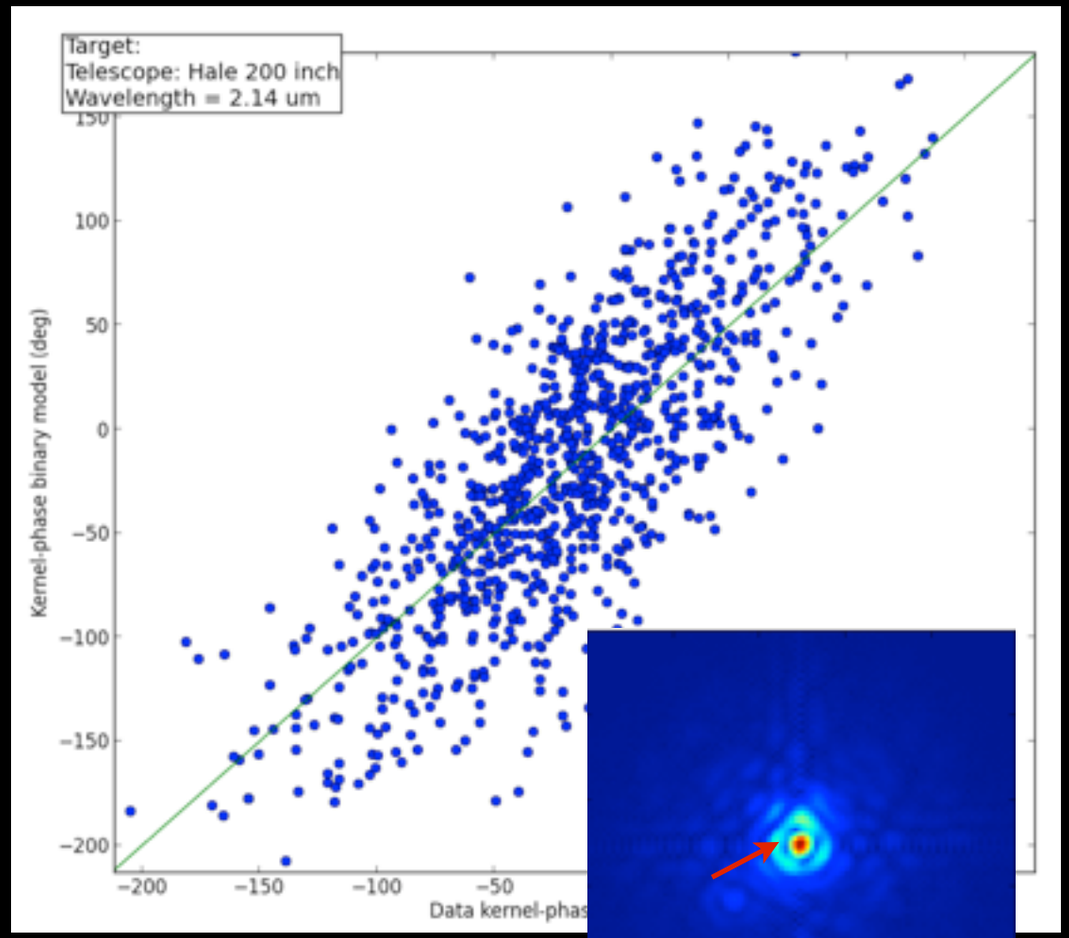

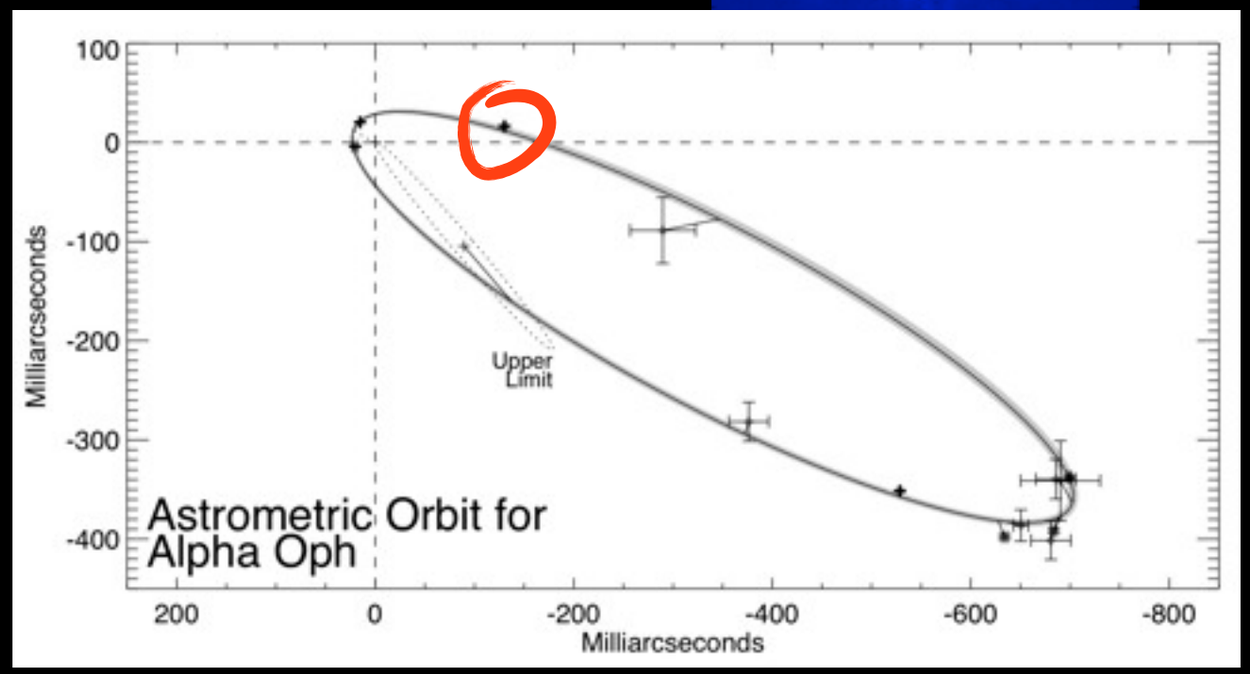

Hinkley et al, 2011, ApJ, 726, 104

Re-analysis of NICMOS I data

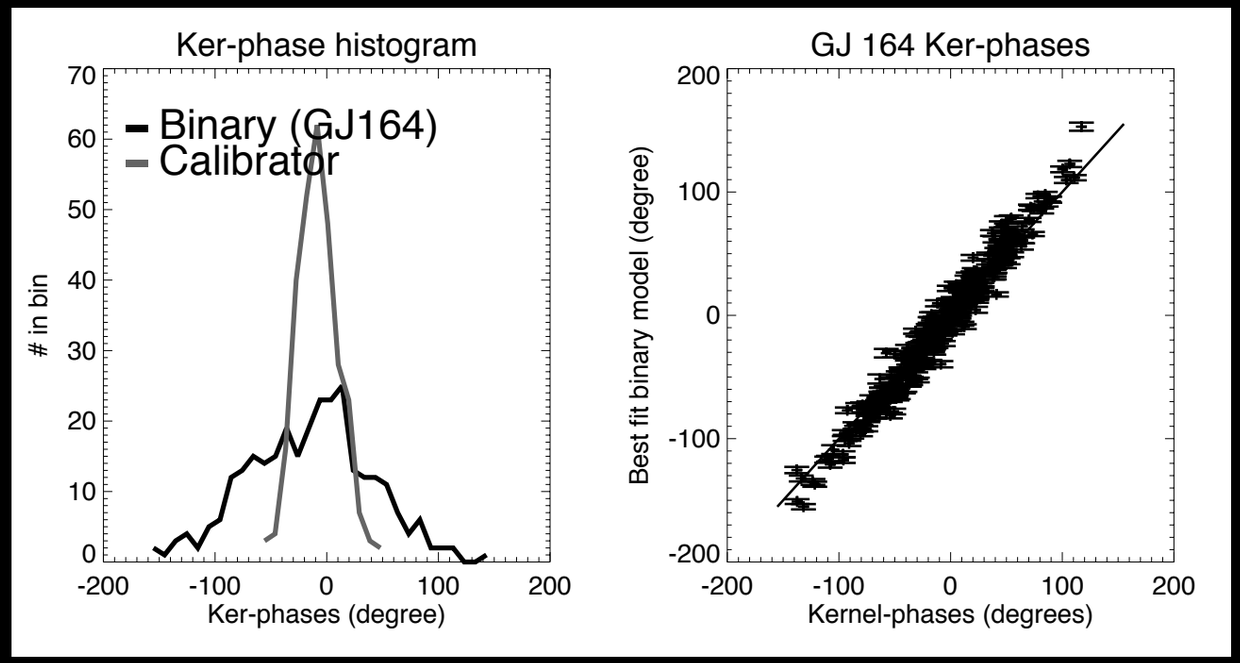

Data @ 1.9 µm (λ/D=150 mas)

A ~10:1 contrast companion to a nearby M-dwarf identified with **milli-arc-second precision** at **0.5 λ/D**

Martinache, 2010, ApJ, 724, 464

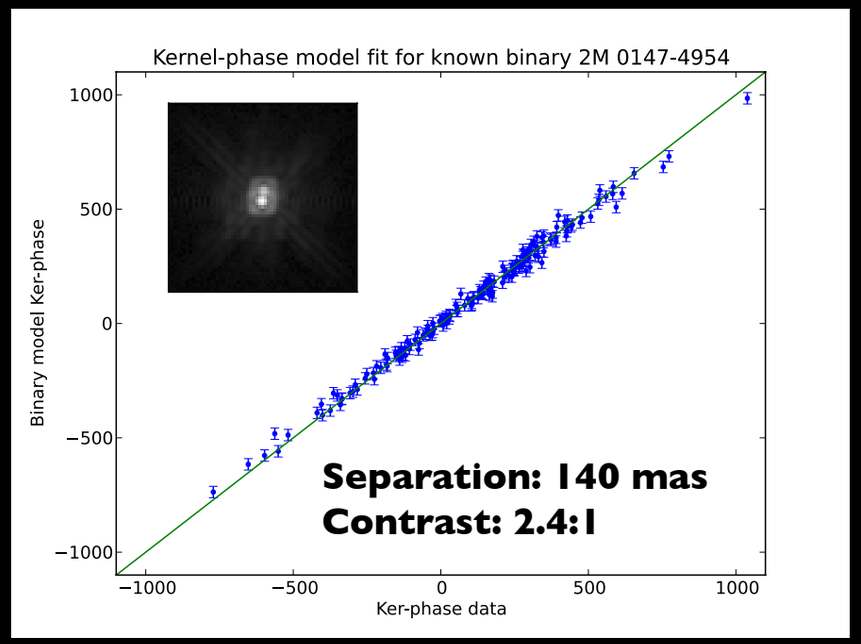

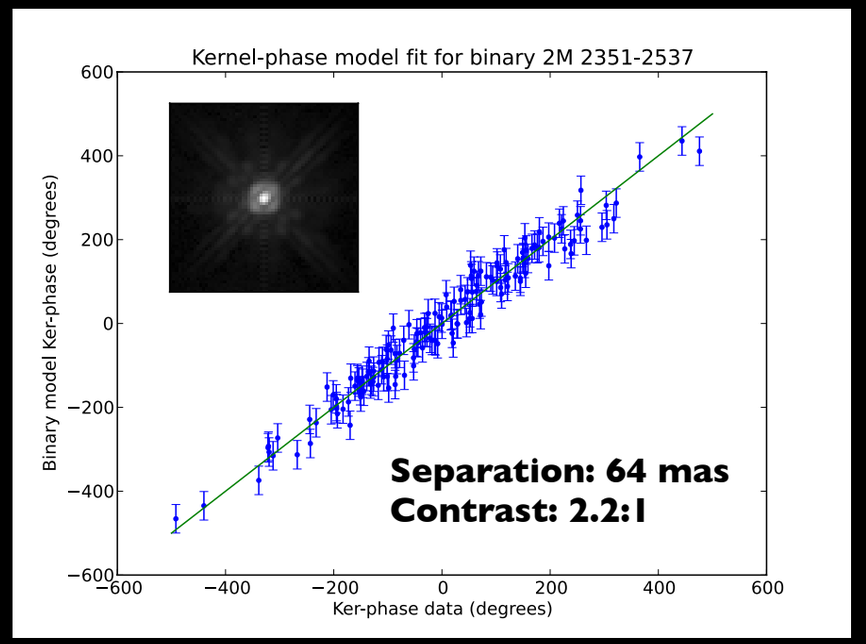

Original survey:
Reid et al, 2006, 2008

Revisit ~ 80 brown dwarfs observed with HST/NIC1 in the F110W and F170M filters

- Doubled the fraction of known L-dwarf binary systems
- Improved astrometry x10

Grant HST-AR-12849.01-A

Pope et al, 2013, ApJ, 767, 110

Better than the kernel-phase...

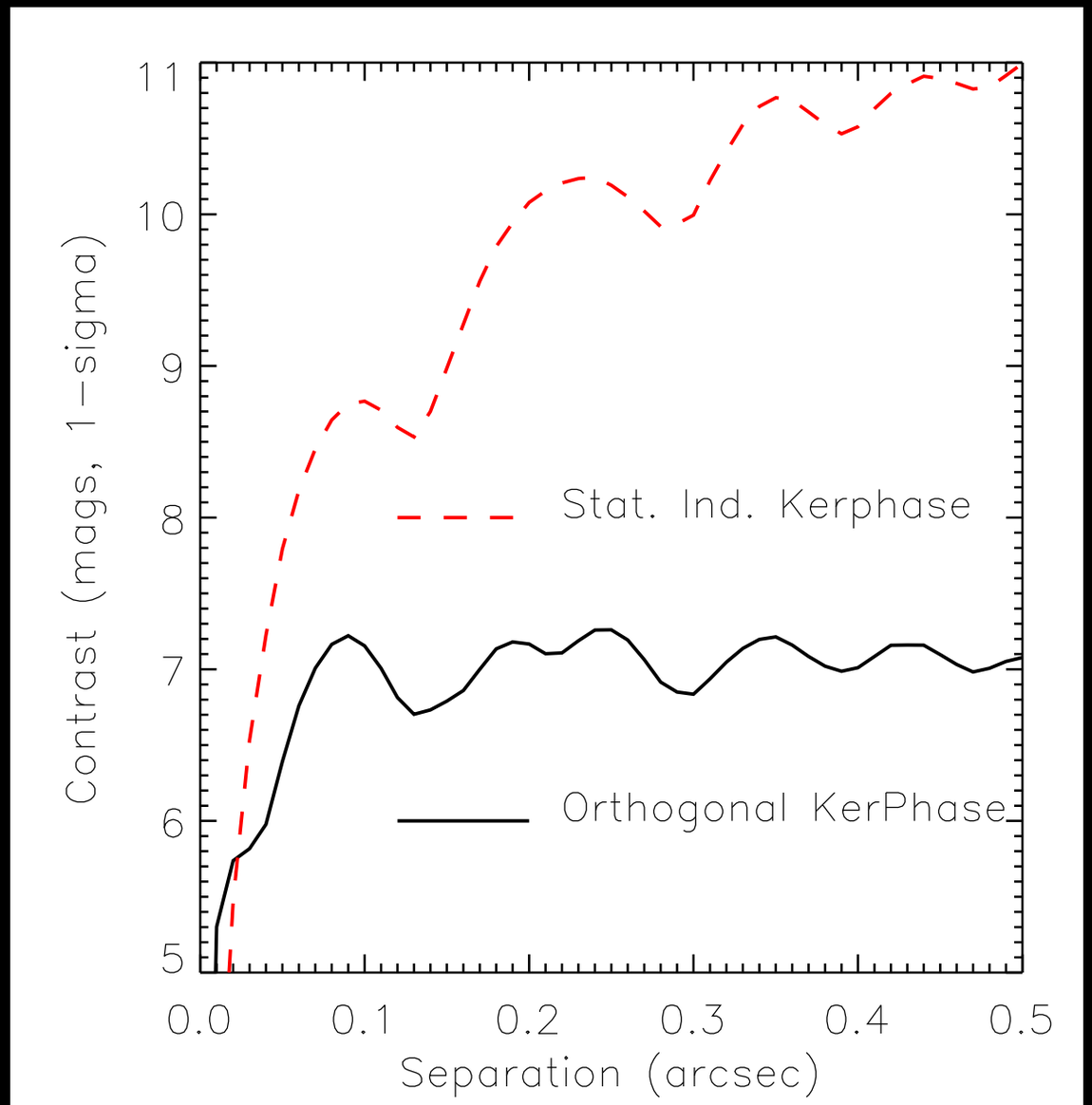

... are the statistically independent kernel-phases!

$$\theta = S.K.\phi$$

Ireland, 2013, MNRAS, 433, 1718

Requires empirical covariance matrices
Part of a new file exchange standard?

Are new observables really required for VLBI?

black and white

From I2T to multi-beam combiner

color!

Tactical benefit:
orthogonal, statistically independent observables are the best for model fit & image reconstruction

Interferometric imaging with rich aperture

NRM geometry: Golay 12

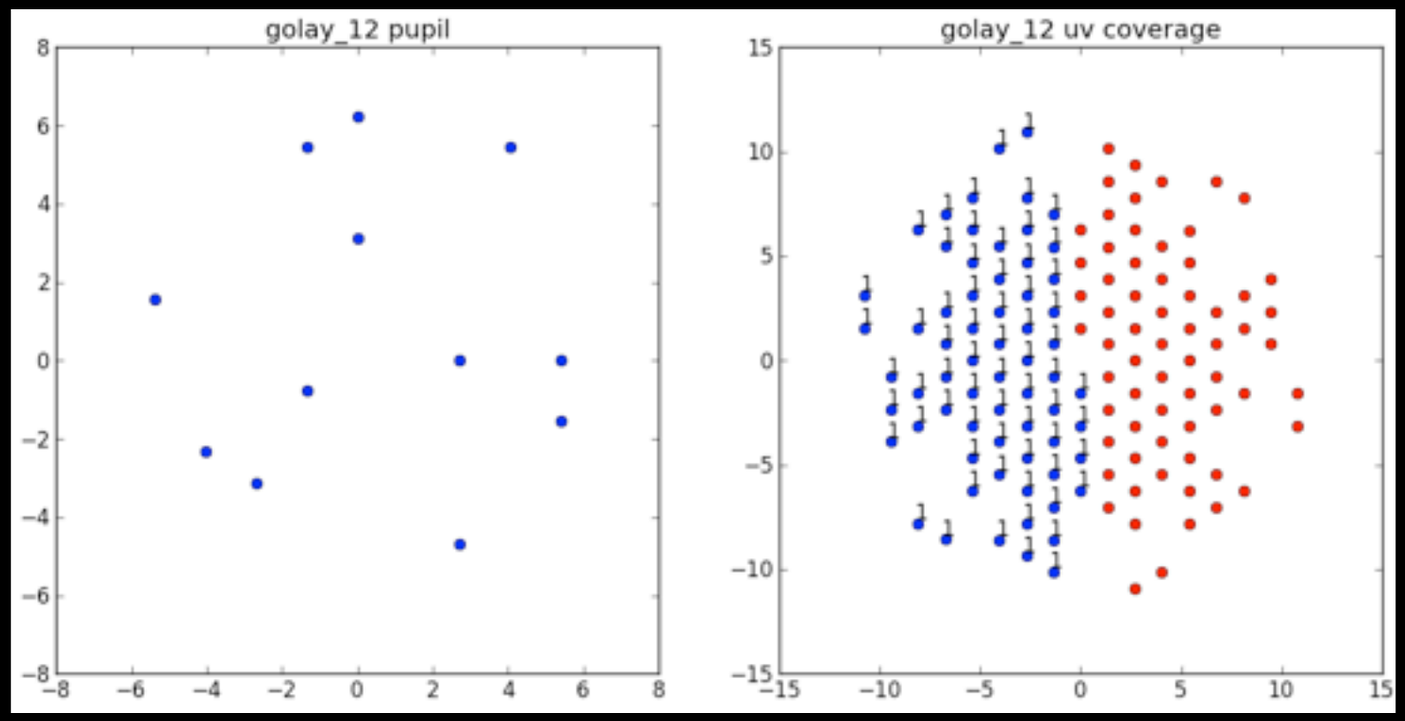

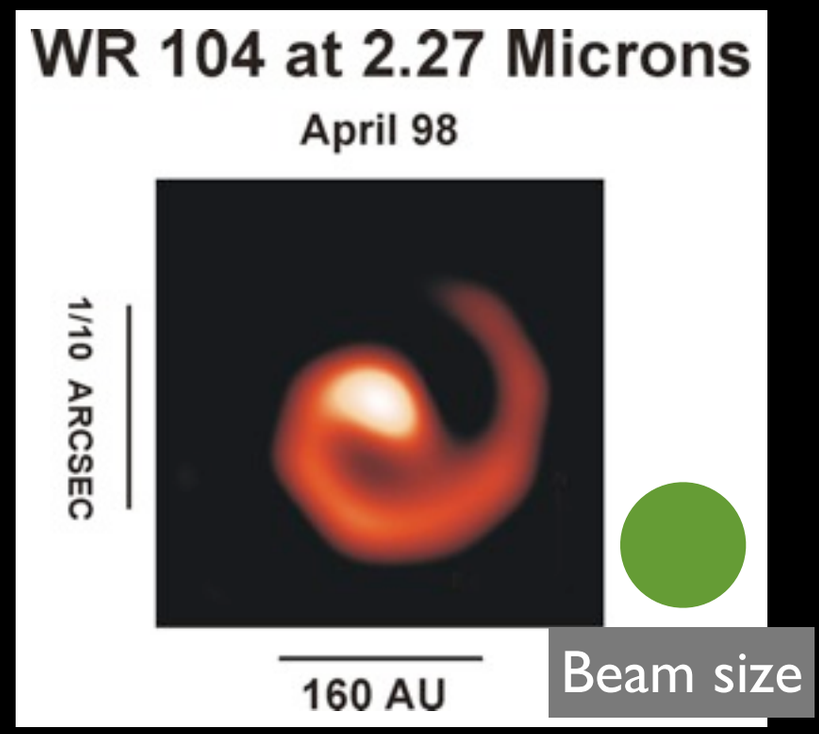

Tuthill et al, 1999, Nature, 398, 487

With kernel-phase, you are no longer constrained by non redundancy rules

Full aperture vs annulus

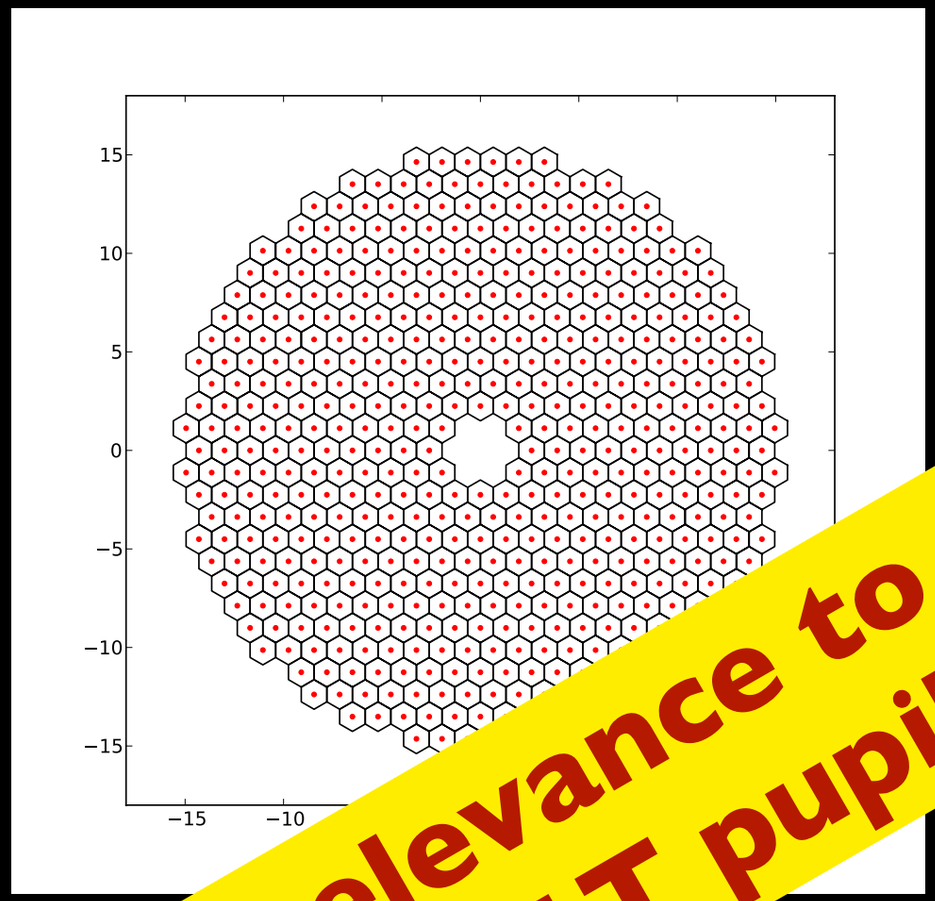

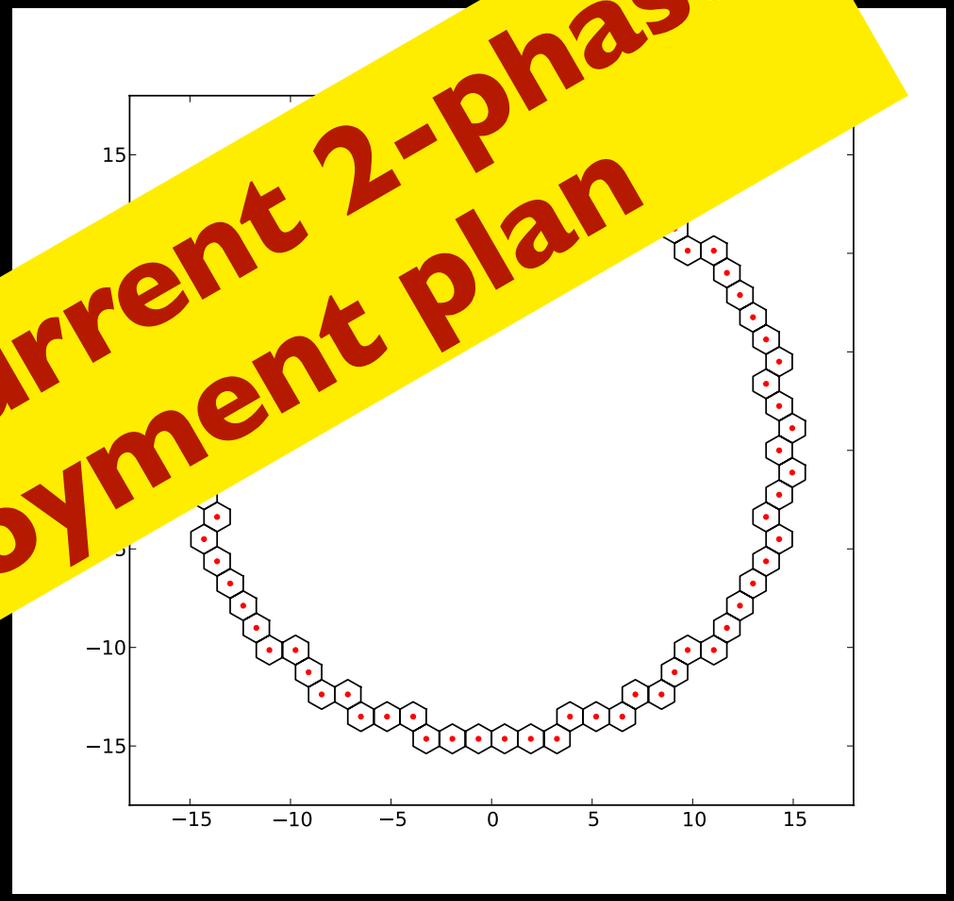

Of relevance to the current 2-phase E-ELT pupil deployment plan

...tial frequencies
...8 kernel-phases (75 %)
Max redundancy: 462
Mean redundancy: 124

78 segments used
972 spatial frequencies
933 kernel-phases (96 %)
Max redundancy: 26
Mean redundancy: 3

Martinache, 2012, SPIE, 8445, 04

Enough information for direct inversion?

In doing:

$K\,\phi = K\,\phi_o + K\,A\,\varphi$

$K\,\phi = K\,\phi_o$

with a well designed array
> 95 % of the phase
information is preserved:
a pseudo inverse K^{-1}
works:

$$\phi_o' = K^{-1}\,K\,\phi$$

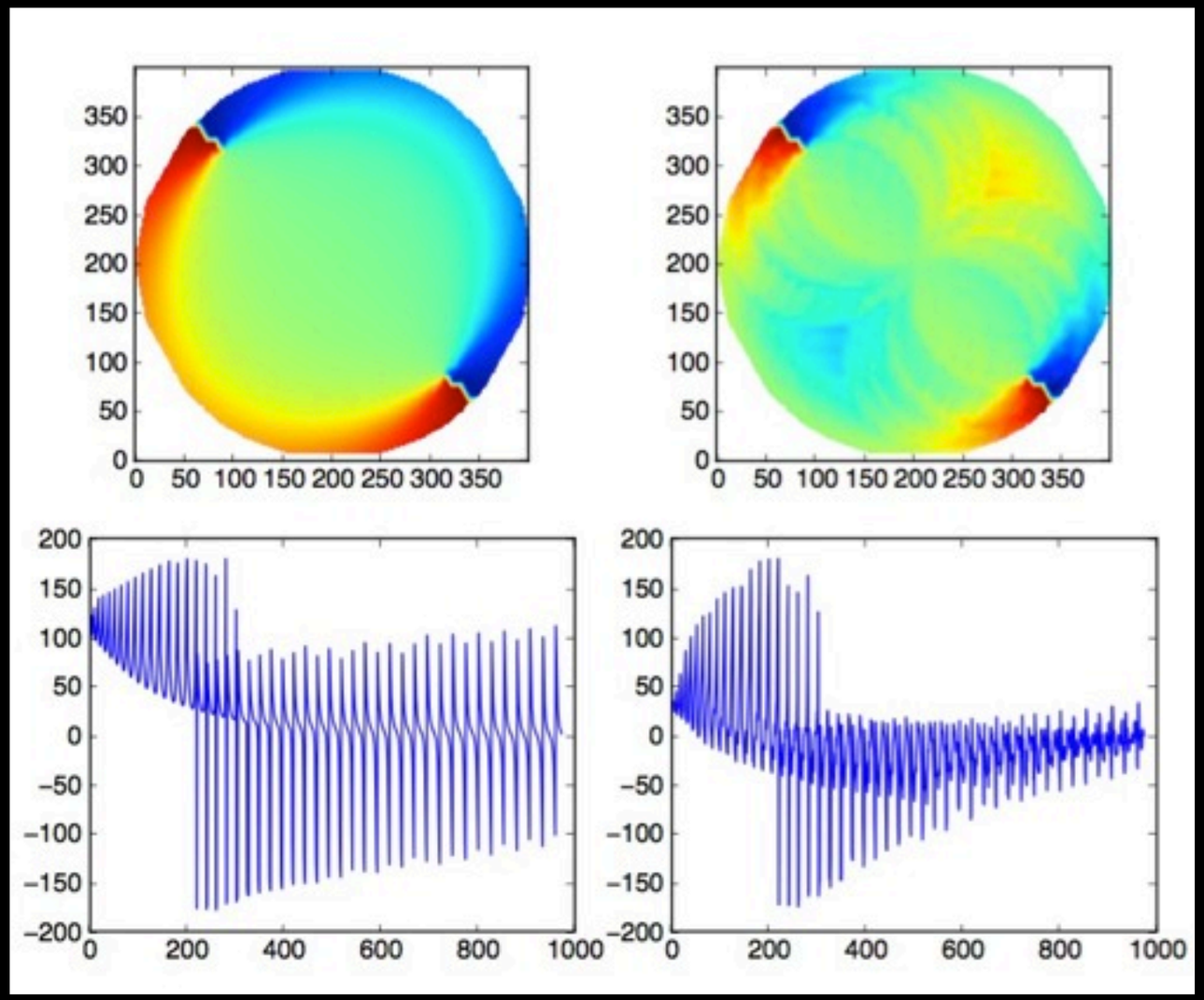

true uv-phase

True phase map

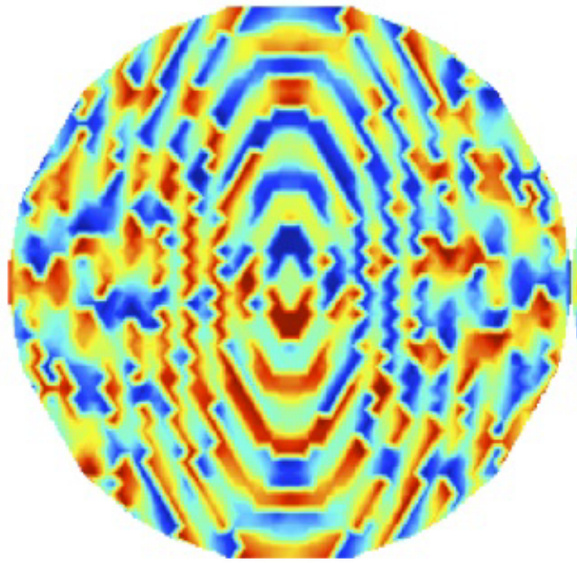

reconstructed uv-phase

Pseudo-inverse phase map

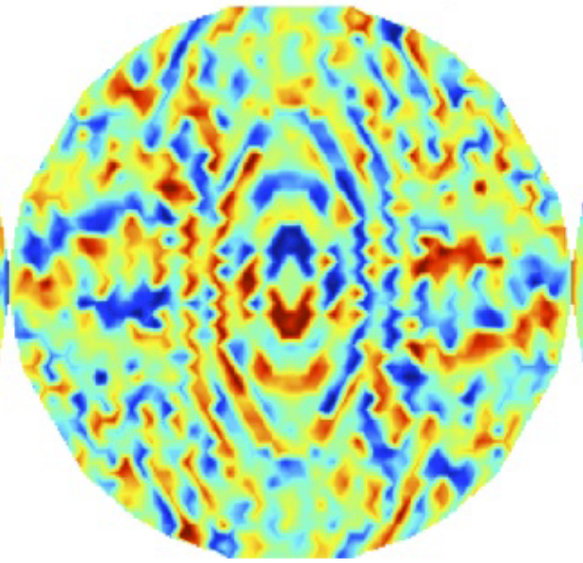

reconstruction error

Difference

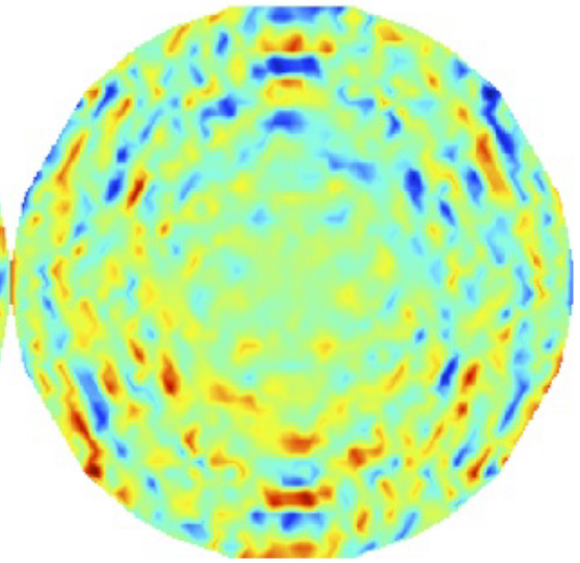

kernel-phase image

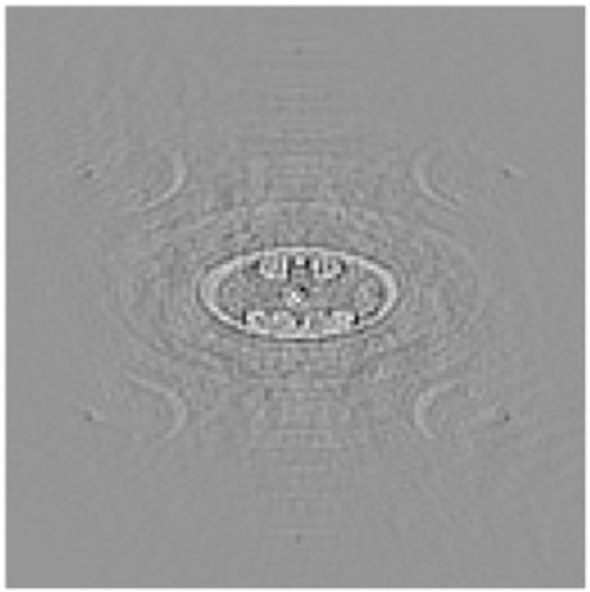

True phase map

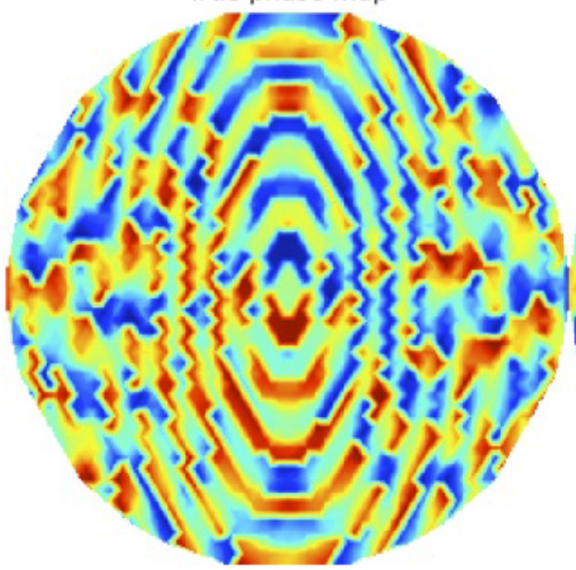

Pseudo-inverse phase map

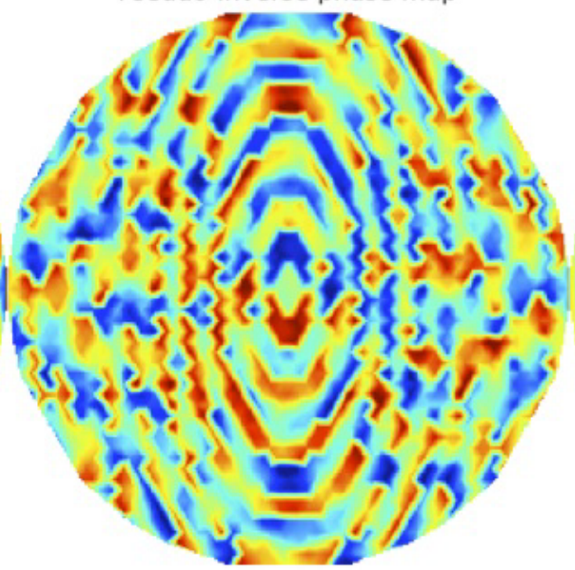

Difference

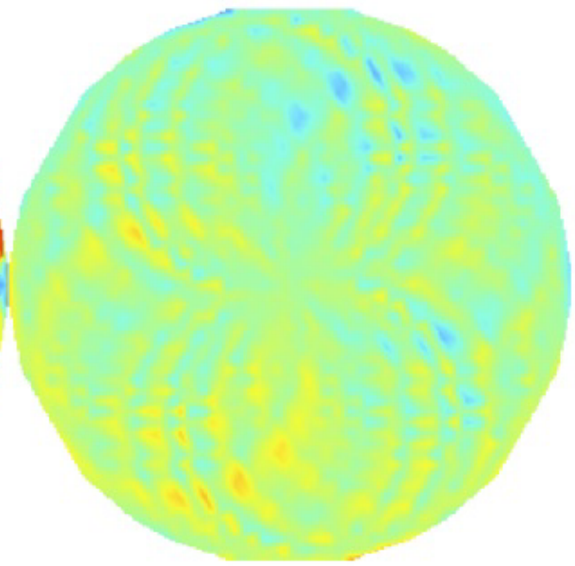

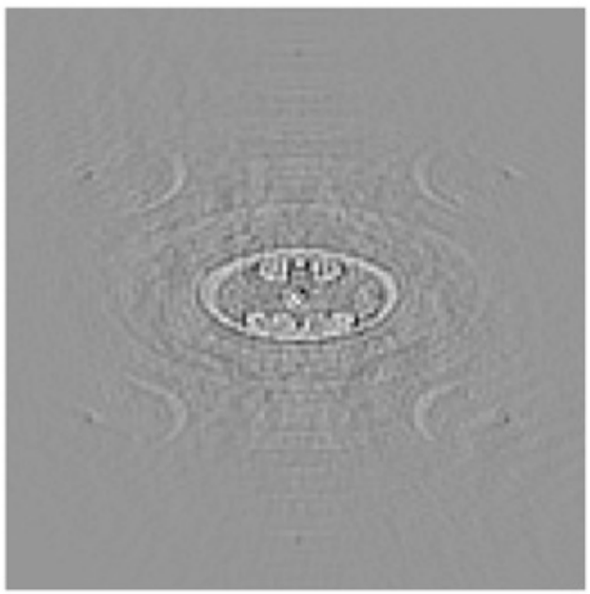

Non-parametric image reconstruction from kernel-phase

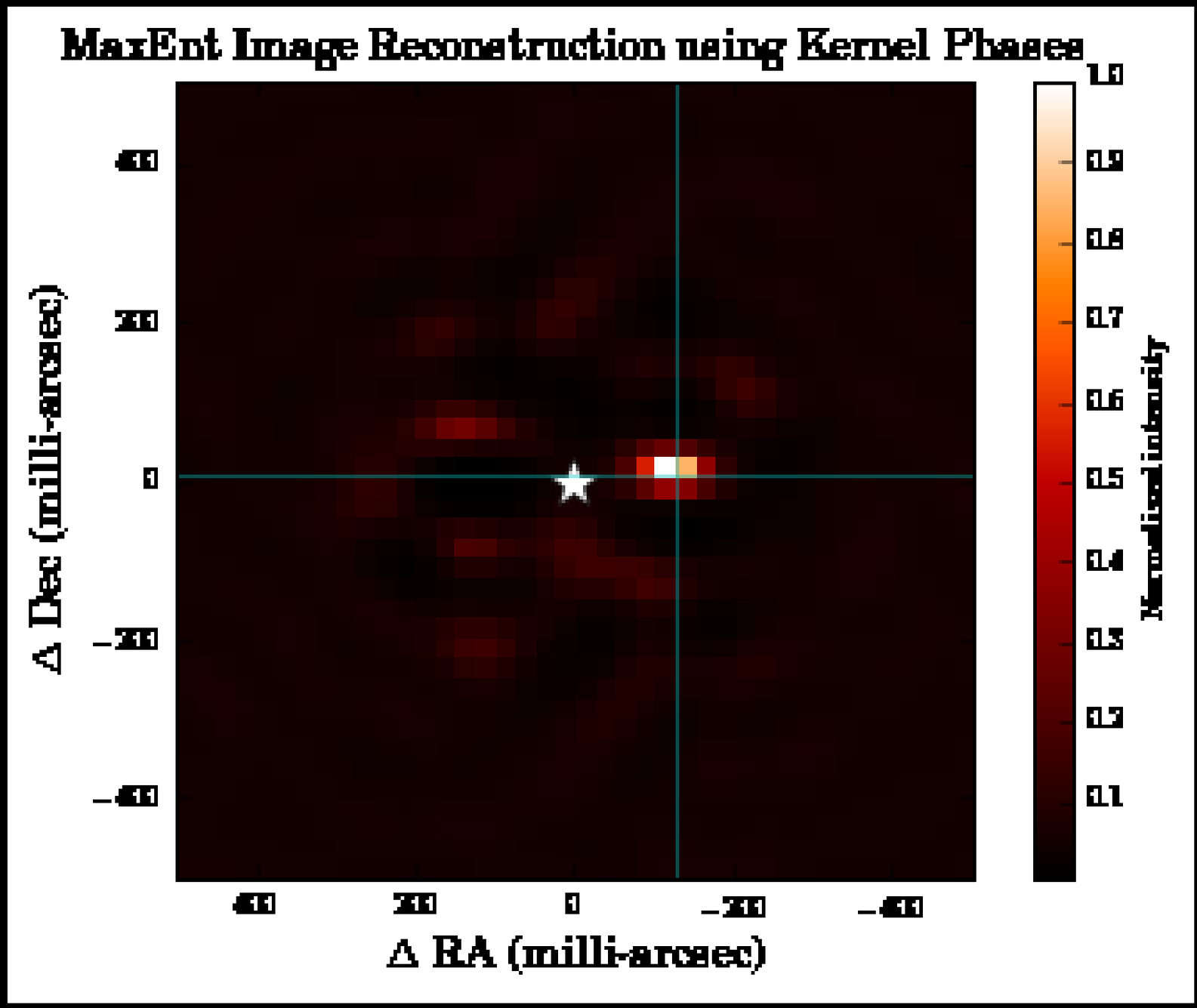

Pope et al, 2015, in prep

Initial assumptions revised

Linear approximation relies on small phase errors

Extensive simulations suggest kernel-phase on highly redundant aperture is quite robust.

	B	C	D	E	F	G	H	I	J	K	L	M
30	Hexagonal	ann_hex15	78	378	339	258.4 (27.31)	21.1 (9.15)	0.463		47.0 (7.38)	250.9 (30.59)	162.3 (15
31	Hexagonal	ann_hex15_w05	48	378	354	152.3 (17.61)	1.0 (0.0)	0.783		26.1 (4.42)	138.0 (13.16)	77.0 (12
32		golay9	9	36	28	38.7 (2.84)	1.0 (0.0)	0.839		5.8 (0.0)	10.5 (0.99)	10.7 (2
33	hases)					41.6 (2.92)				48.8 (4.18)	50.6 (4.45)	39.8 (3
34												
35												
36						Unwrapping off, no low freqs		Kernel phases mean STE (degrees)				
37	Hexagonal	full_hex15	199	378	279	2390.3 (232.92)	2497.2 (829.78)	0.060		1369.9 (146.51)	2606.9 (236.4)	2282.0 (228
38	Hexagonal	ann_hex15	78	378	339	1090.9 (101.93)	423.1 (82.32)	0.113		389.7 (41.32)	1128.3 (113.88)	738.2 (70
39	Hexagonal	ann_hex15_w05	48	378	354	574.4 (43.15)	106.5 (30.67)	0.214		77.4 (12.26)	582.7 (56.53)	277.3 (22
40		golay9	9	36	28	263.9 (16.33)	81.9 (7.55)	0.131		11.1 (0.0)	49.1 (4.15)	28.6 (4
41	hases)					258.5 (12.89)				315.2 (17.1)	332.7 (27.84)	256.1 (14
42												
43												
44						Unwrapping off, no low freqs		Kernel phases mean STE (degrees)				
45	Hexagonal	full_hex15	199	378	279	8771.0 (866.51)	12000.0 (0.0)	0.019		7633.7 (803.44)	9122.4 (867.86)	8373.9 (892
46	Hexagonal	ann_hex15	78	378	339	2959.7 (311.48)	3042.9 (833.78)	0.042		2855.7 (279.82)	2907.7 (303.09)	2891.1 (297
47	Hexagonal	ann_hex15_w05	48	378	354	1302.6 (98.27)	614.4 (227.31)	0.097		1019.8 (78.13)	1256.8 (106.3)	1281.8 (115
48		golay9	9	36	28	1118.2 (93.88)	1500.8 (137.97)	0.031		353.5 (30.06)	1271.5 (93.69)	451.8 (24
49	hases)					1117.4 (91.18)				1266.7 (117.26)	1226.7 (106.74)	1103.5 (70
50												
51												
52						Unwrapping off, no low freqs		Kernel phases mean STE (degrees)				
53	Hexagonal	full_hex15	199	378	279	29032.4 (2887.38)	60000.0 (0.0)	0.007		23625.8 (2416.89)	28447.8 (2872.13)	27539.8 (282
54	Hexagonal	ann_hex15	78	378	339	7815.5 (746.96)	19985.6 (6036.75)	0.017		7074.4 (710.34)	7265.1 (715.55)	7480.7 (705
55	Hexagonal	ann_hex15_w05	48	378	354	3181.9 (257.52)	3558.4 (1326.78)	0.041		2936.5 (255.59)	2961.4 (268.7)	3060.9 (251
56		golay9	9	36	28	4549.0 (567.43)	22009.5 (4197.5)	0.008		4036.9 (553.65)	3953.2 (566.54)	4392.3 (642
57	hases)					4489.0 (489.42)				4236.3 (460.92)	4357.9 (501.39)	4525.2 (627
58												
59												
60						Unwrapping off, no low freqs		Kernel phases mean STE (degrees)				
61	Hexagonal	full_hex15	199	378	279	66290.3 (6418.11)	120000.0 (0.0)	0.003		53702.4 (5750.76)	65668.3 (6231.02)	62210.4 (673
62	Hexagonal	ann_hex15	78	378	339	16961.7 (1602.45)	94086.3 (24825.23)	0.008		15897.5 (1687.9)	16171.1 (1669.26)	16784.8 (169
63	Hexagonal	ann_hex15_w05	48	378	354	6903.4 (554.81)	17871.1 (6679.32)	0.019		6626.6 (507.53)	6726.1 (545.03)	6850.5 (604
64		golay9	9	36	28	10548.3 (1482.8)	30000.0 (0.0)	0.003		9682.9 (1253.02)	9714.3 (1173.27)	10689.0 (156
65	hases)					10870.2 (1501.84)				10322.8 (1365.58)	10090.1 (1486.06)	10890.0 (141

Latyshev, et al, 2015, in prep

Possible example of extension:

Original linearization for small instrumental phase:

$\Phi_j = \Phi_{0j} + \mathrm{Arg}(\Sigma e^{j\,\Delta\varphi i})$ → $\Phi_j = \Phi_{0j} + 1/n_j\, \Sigma_i\, \Delta\varphi i$

alternate linear[illegible]n scheme:

Work in progress

$\Phi_j(\lambda) = \Phi[illegible] \mathrm{Arg}(\Sigma\, \exp(i2\pi\delta/\lambda))$

$\mathrm{Arg}\,(\gamma_j(\lambda_1) \times \gamma^*_j(\lambda_2)) = \Delta\Phi_0(\lambda_1,\lambda_2) + 1/n\, \Sigma\, [2\pi\delta_j/\Lambda_0]$

The same linear model holds for differential phase
Possible applications: visible ELT camera?

kernel-phase for high angular resolution

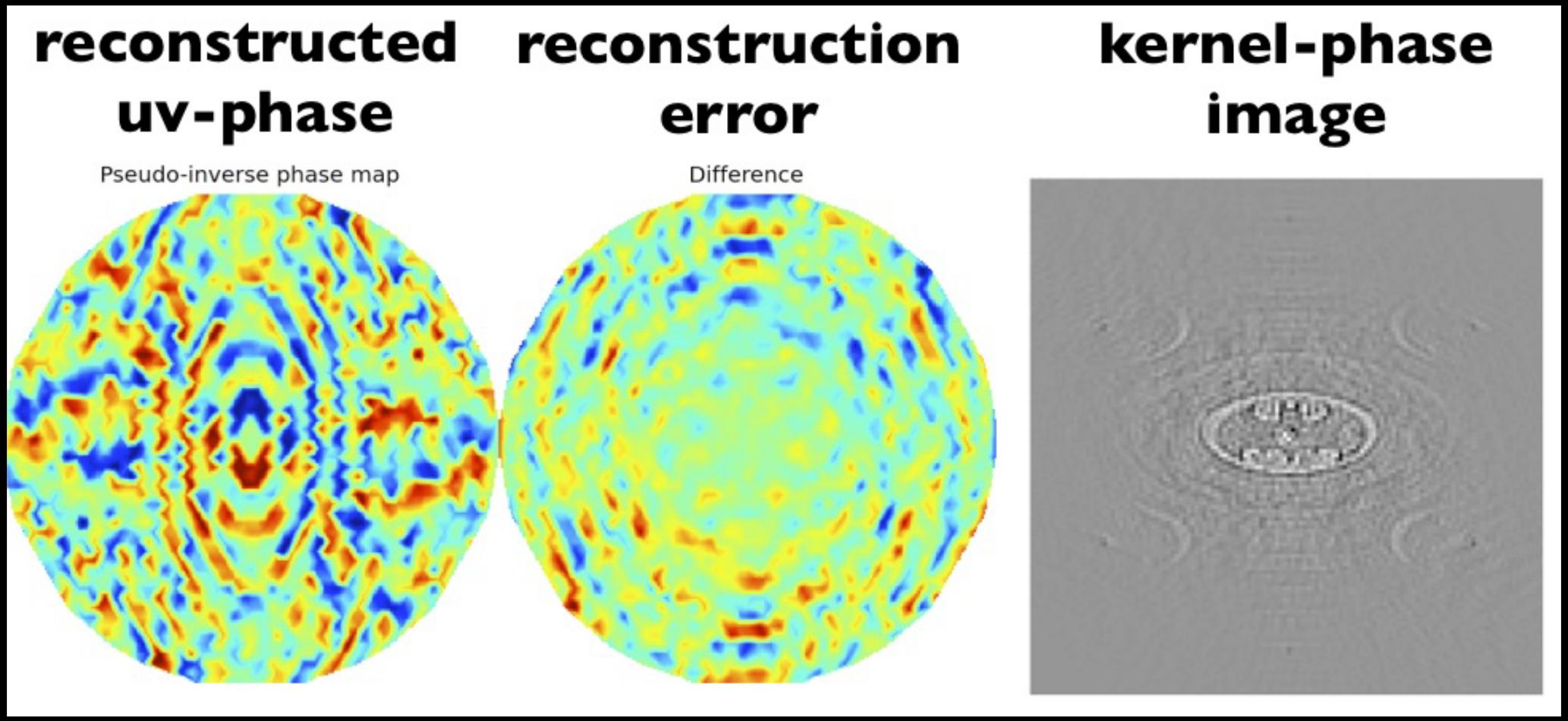

Frantz Martinache, Laboratoire Lagrange, OCA

+ B. Pope, P. Tuthill, M. Ireland, A. Cheetham, A. Latyshev, J. Monnier...

non-redundant triangular array	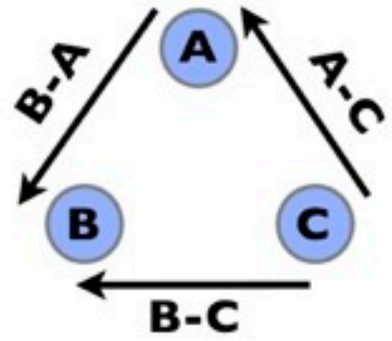	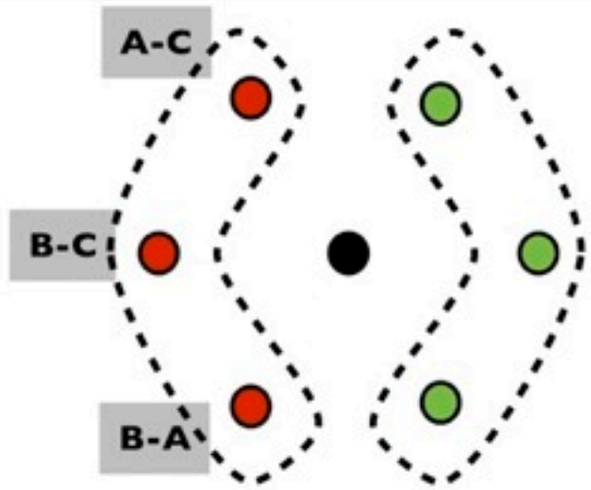
redundant linear array	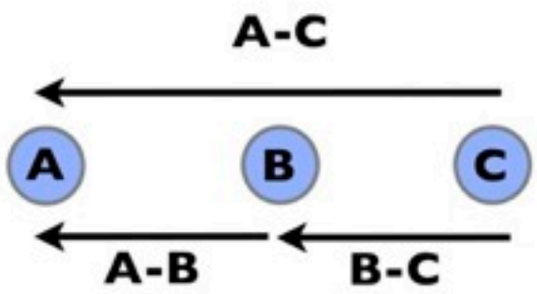	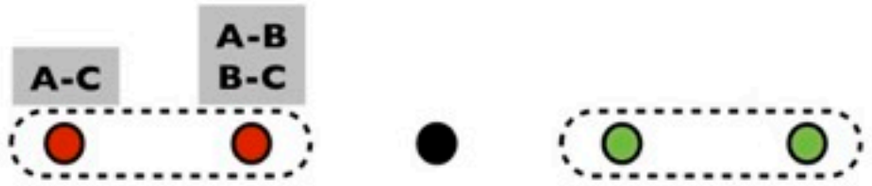
redundant square grid array